INFORMATION TO USERS

This manuscript has been reproduced from the microfilm master. UMI films the text directly from the original or copy submitted. Thus, some thesis and dissertation copies are in typewriter face, while others may be from any type of computer printer.

The quality of this reproduction is dependent upon the quality of the copy submitted. Broken or indistinct print, colored or poor quality illustrations and photographs, print bleedthrough, substandard margins, and improper alignment can adversely affect reproduction.

In the unlikely event that the author did not send UMI a complete manuscript and there are missing pages, these will be noted. Also, if unauthorized copyright material had to be removed, a note will indicate the deletion.

Oversize materials (e.g., maps, drawings, charts) are reproduced by sectioning the original, beginning at the upper left-hand corner and continuing from left to right in equal sections with small overlaps.

ProQuest Information and Learning
300 North Zeeb Road, Ann Arbor, MI 48106-1346 USA
800-521-0600

Fault Tolerant Control for Aircraft Control Surface Failures

By

Abderrazak Idrissi Belkharraz

A dissertation submitted to the Graduate

Faculty in Engineering in fulfillment of

the requirements for the degree of

Doctor of Philosophy,

The City University of New York

2003

This manuscript has been read and accepted for the Graduate Faculty in Engineering in satisfaction of the dissertation for the degree of Doctor of Philosophy.

July 9, 2003
Date

Kenneth Sobel
Chair of Examining Committee

July 9, 2003
Date

Mumtaz K. Kassir
Executive Officer

Professor K.M. Sobel, Mentor

Professor F.E. Thau

Professor G.M. Kranc

Professor J. Xiao

Dr. J.E. Piou, MIT Lincoln Lab

Supervisory Committee

The City University of New York

Abstract

Fault Tolerant Control for Aircraft Control Surface Failures

By

Abderrazak Idrissi Belkharraz

Adviser: Professor Kenneth M. Sobel

In recent years, fault tolerant flight control systems have gained an increased interest for high performance military aircraft as well as civil aircraft. Fault tolerant control systems can be described as either active or passive. An active fault tolerant control system has to either reconfigure or adapt the controller in response to a failure. In contrast, a passive fault tolerant control system uses a fixed controller which achieves acceptable performance for a presumed set of failures.

A passive fault tolerant flight control law is designed for the F/A-18 aircraft which achieves acceptable handling qualities for a class of control surface failures. The class of failures includes the symmetric failure of any one control surface being stuck at its trim value. A comparison is made of an eigenstructure assignment gain designed for the unfailed aircraft with a fault tolerant multiobjective optimization gain. We show that the time re-

sponses for the unfailed aircraft using the eigenstructure assignment gain and the fault tolerant gain are identical. Furthermore, the fault tolerant gain achieves MIL-F-8785C specifications for all failure conditions.

An active fault tolerant control law is designed by using direct model reference adaptive control for multi-input multi-output plants. We augment the plant with a feedforward compensator such that the inverse feedforward stabilizes the plant over the set of allowable failures. We prove that the augmented output error is asymptotically vanishing for a loss of control effectiveness failure. A novel state space approach for computing the feedforward compensator is proposed. We demonstrate the use of our algorithm by application to a three input model of the linearized lateral dynamics of the F/A-18 aircraft.

Acknowledgments

To Prof. K.M. Sobel, a mentor who takes his job with honesty, seriousness, and love, whose guidance was so crucial in the realization of this work. I learned from him patience, excellence, and quality. He did everything possible to make my dream come true. Prof. Sobel, I am very greatful.

I would like to express my sincere gratitude to Dr. J.E. Piou from MIT Lincoln Lab for his valuable assistance, comments, and feedback especially with respect to proofs of theorems and lemmas.

A special thank you to Profs. F. Thau and G. Kranc for their advice, training, and support during this rewarding period at the E.E Department of The City College of New York.

To my father Mustapha Belkharraz who passed away in 1994. I never felt he is as alive as I feel it at this moment. To him I dedicate this degree as a thank you for just being my father. To my beloved mom Zoubida who despite the distance, I could hear her prayers and feel her love whenever I needed them.

To everyone who truly supported me through these difficult moments of my life.

Contents

List of Tables

List of Figures

Chapter 1

Introduction

1.1 Background

Aircraft flight control systems are designed with extensive redundancy to ensure a low probability of failure. During recent years, however, several aircraft have experienced major control system failures. These failures have caused an increased interest in fault tolerant flight control systems. The objective of fault tolerant flight control is to control and safely land the aircraft in case of severely damaged or inoperable control surfaces. The two approaches to fault tolerant control are active and passive control. An active fault tolerant control system has to either reconfigure or adapt the controller in response to the failure. One way is to reconfigure the controller

based upon detection and identification of the failure. Another way is to use direct adaptive control to adjust the controller without explicitly identifying the failure. In contrast, a passive fault tolerant control system uses a fixed controller which achieves acceptable handling qualities for a given set of failures.

1.1.1 Eigenstructure Assignment Methods

Several authors have utilized eigenstructure assignment to design reconfigurable flight control systems. Gavito and Collins [1] used eigenstructure assignment to recover the undamaged modal response under the assumption that the failure has been detected and identified. Napolitano and Swaim [2] used eigenstructure assignment to remove the lateral-longitudinal coupling induced by an asymmetric control surface failure. Jiang [3] used eigenstructure assignment to recover the dominant eigenvalues and eigenvectors of an aircraft longitudinal control system which has undergone some operating condition variations or system component failures. However, all of these approaches require an on-line identification of the parameters of the plant after failure.

Jiang and Zhao [4] used eigenstructure assignment to design passive fault

tolerant controllers for actuator failures. This approach is based on robust regional eigenvalue assignment with the addition of a precompensator. However, this design method requires extensive redundancy. Gorrec et. al. [5] proposed a multimodel approach for the landing phase of a large transport aircraft. This method uses a bank of models covering the entire flight envelope. First, the authors design an initial gain for a chosen original model. This gain is used to control all of the models and a multimodel analysis is used to detect the worst model. Then, a quadratic optimization procedure is used to improve the behavior of the worst model while keeping good performance relative to the original model. However, the designer must be careful to avoid conflicting objectives.

Our first contribution is a new result for eigenstructure invariance when it is known which control surface is most likely to fail. We seek a constant gain output feedback controller such that the dominant eigenstructure is invariant under this failure. We show mathematically that the solution is that the failed control surface should not be used. That is, if the j^{th} control surface will fail, then the j^{th} row of the constant output feedback gain matrix will be simply zero. For this purpose, we first derive a basis for the subspace in which the eigenvectors of the failed system must lie. Then, we show that

there exists a constant output feedback gain matrix which yields an invariant dominant eigenstructure both before and after failure. Finally, we prove that the j^{th} row of this feedback gain matrix will be zero.

Our second contribution is the design of a passive fault tolerant flight controller for a control surface failure. We consider the linearized lateral dynamics of the F/A-18 aircraft. The class of control surface failures we consider includes the symmetric failure of any one control surface being stuck at its trim value. It is not known in advance which control surface will fail. We compute an optimal feedback gain using an off-line multiobjective optimization technique. A comparison is made of an eigenstructure assignment gain designed for the unfailed aircraft with the fault tolerant multiobjective optimization gain. We show that the time responses for the unfailed aircraft using the eigenstructure assignment gain and the fault tolerant gain are identical. Furthermore, the fault tolerant gain achieves MIL-F-8785C specifications for all failure conditions.

1.1.2 Adaptive Control Methods

Model reference adaptive control is based upon matching the response of a system or "plant" to that of a reference model. The inputs to the plant

(which are generated from the model inputs, the model states, and the error between plant and model outputs) drive the outputs of the plant to equal the outputs of the model.

Boskovic and Mehra [6] designed an adaptive control reconfiguration scheme for accommodation of actuator failures for a class of plants where the number of control inputs is larger than the number of measurements. Ref. [6] uses an adjustable adaptive control law to achieve the control objective based on the overall system response. Hence, no failure detection and identification is needed. However, the state of the system is required to be available. Later, Boskovic and Mehra [7] proposed a multiple model based reconfigurable flight control for an advanced fighter aircraft in the presence of wing damage. This method is based on the concept of multiple models, switching, and tuning. Ref. [7] includes an output error feedback term in the controllers. This makes the overall system robust when the actual damage does not coincide with any of the models. However, the system becomes sensitive to noise. Furthermore, the plant is assumed to be invertible, minimum phase, and full state feedback is required. More recently, Boskovic and Mehra [8] proposed an intelligent adaptive reconfigurable control scheme to improve the method described in Ref. [7]. This scheme uses multiple ob-

servers to find the reference model closest to the current plant dynamics and switches to the corresponding controller. However, the plant is still required to be invertible, minimum phase, and full state feedback is required. In their latest work, Boskovic and Mehra [9] proposed a multiple model adaptive control to accommodate different types of actuator failures. The design uses a parameterization for the actuator failures in terms of input signals and controller gains. This enables the inputs and gains to be estimated separately. Ref. [9] considers locked in place, hard over, and loss of control effectiveness failures. However, the state of the system is still required to be available. Moreover, the number of actuators has to exceed the number of states directly affected by the failure of these actuators.

Tao et. al. [10] proposed an adaptive control algorithm for systems with actuator failures using state feedback. Later, Tao et. al. [11] extended their approach to output tracking. However, the authors require that matching conditions be satisfied. In general, these conditions are restrictive and the design is applicable only to single output plants.

Kaufman et. al. [12] have developed direct adaptive control algorithms for multiple input multiple output systems. Stability is proven for plants that

are almost strictly positive real (ASPR) for all possible plant parameter values. In Ref. [12] the authors insert a feedforward compensator around the plant so that the augmented system is ASPR. Ref. [12] presents time and frequency domain approaches for designing the feedforward compensator. The time domain approach is based upon satisfying constraints which ensure the stability of the characteristic polynomial of the closed loop system for all possible parameter variations. The frequency domain approach is based upon modeling the plant uncertainty as either additive or multiplicative perturbations in the transfer function matrix.

Morse and Ossman [13] applied the algorithms of Ref. [12] to reconfigurable flight control of the AFTI/F-16 aircraft. However, Morse and Ossman [13] assume that all state variables are measurable which significantly simplifies the controller design.

Our third contribution is a new result for direct adaptive control of multi-input multi-output systems with control surface failures. We augment the plant with a feedforward compensator such that the inverse feedforward stabilizes the plant over the set of allowable failures. We prove that the augmented output error is asymptotically vanishing for loss of control ef-

fectiveness failures. A novel state space approach for computing the feedforward around the plant is proposed. We use the MATLAB® LMI Toolbox [14] and the MATLAB® Optimization Toolbox [15] to find a feedback gain K which (1) stabilizes the plant for all possible failure configurations and (2) minimizes the inverse of the gain K. Then, the feedforward gain K^{-1} achieves the ASPR condition for all failure configurations. We demonstrate the use of our algorithm by application to a three input model of the linearized lateral dynamics of the F/A-18 aircraft.

1.2 Historical Review

1.2.1 Eigenstructure Assignment for Linear Systems

Consider an aircraft modeled by the linear time invariant matrix differential equation described by

$$\dot{x} = Ax + Bu \tag{1.1}$$

$$y = Cx \tag{1.2}$$

where x is the state vector $(n \times 1)$, u the control vector $(m \times 1)$ and y the output vector $(r \times 1)$. It is assumed that the m inputs and the r outputs are

independent. If there are no pilot commands, the control vector u equals a matrix F times the output vector y:

$$u = -Fy \tag{1.3}$$

Theorem 1.1 *[16]*

Given the controllable and observable system described by Eqs. (1.1) and (1.2), $max(m,r)$ closed loop eigenvalues can be assigned and $max(m,r)$ eigenvectors (or reciprocal vectors by duality) can be assigned with $min(m,r)$ entries in each vector arbitrarily chosen using constant output feedback.

Andry et. al. [17] concluded that the eigenvectors v_i must be in the subspace spanned by the columns of $(\lambda_i I - A)^{-1}B$. This subspace is of dimension m which is equal to the number of independent control variables. Thus, if we choose an eigenvector v_i which lies precisely in the subspace spanned by the columns of $(\lambda_i I - A)^{-1}B$, it will be achieved exactly. In general, however, a desired eigenvector v_i^d will not reside in the prescribed subspace and hence cannot be achieved.

Ref. [17] describes a method for computing the " best possible choice " for an achievable eigenvector. This best possible eigenvector is the projection of v_i^d onto the subspace spanned by the columns of $(\lambda_i I - A)^{-1}B$ (in the

least square sense). In many practical situations, complete specification of v_i is neither required nor known, but rather the designer is interested only in certain elements of the eigenvector. Thus, assume that v_i has the following structure:

$$v_i^d = [v_{i1}, \mathrm{x}, \mathrm{x}, \mathrm{x}, \mathrm{x}, v_{ij}, \mathrm{x}, \mathrm{x}, v_{in}]^T$$

where v_{ij} are designer specified components and x is an unspecified component. Define, as shown by Andry et. al. [17], a reordering operation $\{\ \}^{R_i}$ such that

$$\{v_i^d\}^{R_i} = \begin{bmatrix} \ell_i \\ d_i \end{bmatrix} \tag{1.4}$$

where ℓ_i is a vector of specified components of v_i^d and d_i is a vector of unspecified components of v_i^d. The rows of the matrix $(\lambda_i I - A)^{-1}B$ are also reordered to conform with the reordered components of v_i^d. Thus,

$$\{(\lambda_i I - A)^{-1}B\}^{R_i} = \begin{bmatrix} \tilde{L}_i \\ D_i \end{bmatrix} \tag{1.5}$$

Then, as shown by Andry et. al. [17], the achievable eigenvector v_i^a is given by

$$v_i^a = (\lambda_i I - A)^{-1}Bz_i \tag{1.6}$$

where $z_i = \tilde{L}_i^{\dagger}\ell_i$ and where $(\cdot)^{\dagger}$ denotes the appropriate pseudoinverse of $(\cdot)$.

1.2.2 Pseudo Control

Sobel and Lallman [18] proposed a pseudo control strategy for reducing the dimension of the control space by using the singular value decomposition. Once the design is complete the controller is mapped back into the original control space. The following describes the pseudo control strategy.

Consider an aircraft modeled by the linear time-invariant matrix differential equation given by Eqs. (1.1) and (1.2).

Consider the singular value decomposition of the control distribution matrix B given by

$$\begin{aligned} B &= U\Sigma V^T \\ &= \begin{bmatrix} U_3 & U_0 \end{bmatrix} \begin{bmatrix} \Sigma_3 & \\ & 0 \end{bmatrix} \begin{bmatrix} V_3^T \\ V_0^T \end{bmatrix} \end{aligned} \tag{1.7}$$

where U is the matrix of left singular vectors, V is the matrix of right singular vectors, and Σ is a diagonal matrix containing the singular values in the order of descending magnitude.

Suppose we partition the matrix Σ as follows:

$$\Sigma_3 = \begin{bmatrix} \sigma_1 & & & & & \\ & \ddots & & & & \\ & & \sigma_a & & & \\ & & & \sigma_{a+1} & & \\ & & & & \ddots & \\ & & & & & \sigma_b \end{bmatrix} = \begin{bmatrix} \Sigma_1 & \\ & \Sigma_2 \end{bmatrix} \tag{1.8}$$

where

$$\sigma_b \leq \sigma_{b-1} \leq \ldots \leq \sigma_{a+1} < \varepsilon \tag{1.9}$$

with ε not necessarily close to zero. If we partition U_3 and V_3 conformally with Σ_3, then we rewrite Eq. (1.7) as follows:

$$B = \begin{bmatrix} U_1 & U_2 & U_0 \end{bmatrix} \begin{bmatrix} \Sigma_1 & & \\ & \Sigma_2 & \\ & & 0 \end{bmatrix} \begin{bmatrix} V_1^T \\ V_2^T \\ V_0^T \end{bmatrix} \tag{1.10}$$

Now let the system with pseudocontrol δ be described by

$$\begin{cases} \dot{x} = Ax + \tilde{B}\delta \\ y = Cx \end{cases} \tag{1.11}$$

where

$$\tilde{B} = U_1 \tag{1.12}$$

A feedback pseudo control δ is designed for the system described by Eq. (1.11). Then, the true control u for the system described by Eqs. (1.1) and (1.2) is given by

$$u = V_1 \Sigma_1^{-1} \delta \tag{1.13}$$

To derive the inverse control mapping given by Eq. (1.13), we observe that upon comparing Eqs. (1.1) and (1.11), we require

$$Bu = \tilde{B}\delta \tag{1.14}$$

Solving for the true control u, we obtain

$$u = B^{\dagger}\tilde{B}\delta \tag{1.15}$$

where the pseudoinverse $B^{\dagger}$ may be written as [19]

$$B^{\dagger} = V_3 \Sigma_3^{-1} U_3^T \tag{1.16}$$

Upon combining Eqs. (1.12), (1.15), and (1.16) we obtain

$$u = (V_3 \Sigma_3^{-1} U_3^T) U_1 \delta \tag{1.17}$$

Using Eq. (1.10) yields

$$u = \begin{bmatrix} V_1 & V_2 \end{bmatrix} \begin{bmatrix} \Sigma_1^{-1} & \\ & \Sigma_2^{-1} \end{bmatrix} \begin{bmatrix} U_1^T \\ U_2^T \end{bmatrix} U_1 \delta \tag{1.18}$$

Expand Eq. (1.18) to obtain

$$u = V_1 \Sigma_1^{-1} U_1^T U_1 \delta + V_2 \Sigma_2^{-1} U_2^T U_1 \delta \tag{1.19}$$

But, from the properties of the singular value decomposition [19], we have that U and V are unitary matrices. Hence,

$$U_1^T U_1 = I \tag{1.20}$$

and

$$U_2^T U_1 = 0 \tag{1.21}$$

Thus, we obtain the desired result that

$$u = V_1 \Sigma_1^{-1} \delta \tag{1.22}$$

Later, Sobel and Shapiro [20] extended the pseudo control strategy to allow the designer more freedom by adjusting a two dimensional parameter denoted by α. Sobel and Shapiro [20] applied the extended pseudo control strategy to design a yaw pointing/lateral translation control law for the FPCC aircraft.

1.2.3 Model Reference Adaptive Control

Model reference adaptive control is based upon matching the response of a system or "plant" to that of a reference model. The inputs to the plant (which

are generated from the model inputs, the model states, and the error between plant and model outputs) drive the outputs of the plant to equal the outputs of the model. Kaufman et. al. [12] have developed direct adaptive control algorithms for multiple input multiple output systems containing significant uncertainty and disturbances.

1.2.3.1 Basic Algorithm

Consider the plant described by

$$\dot{x}_p(t) = A_p x_p(t) + B_p u_p(t) \tag{1.23}$$

$$y_p(t) = C_p x_p(t) \tag{1.24}$$

where $x_p(t)$ is the plant state vector $(n \times 1)$, $u_p(t)$ the control vector $(m \times 1)$ and $y_p(t)$ the plant output vector $(r \times 1)$, and A_p and B_p are matrices with appropriate dimensions. The plant parameters are assumed to be bounded. The objective is to find without explicit knowledge of A_p and B_p, the control $u_p(t)$ such that the plant output $y_p(t)$ approximates the output of the reference model:

$$\dot{x}_m(t) = A_m x_m(t) + B_m u_m(t) \tag{1.25}$$

$$y_m(t) = C_m x_m(t) \tag{1.26}$$

We emphasize that the order of the plant may be much greater than the order of the reference model.

The adaptive control law [12] that forces the plant output to track the reference model output is given by

$$u_p(t) = K_x x_m(t) + K_u u_m + K_e[y_m(t) - y_p(t)] \tag{1.27}$$

where K_x, K_u, and K_e are adaptive.

The adaptive gains are concatenated into matrix $K_r(t)$ defined as

$$K_r(t) = \left[K_e(t), K_x(t), K_u(t) \right] \tag{1.28}$$

The concatenated gain $K_r(t)$ is defined as the sum of a proportional gain $K_p(t)$ and an integral gain $K_I(t)$, each of which is adapted as follows:

$$K_r(t) = K_p(t) + K_I(t) \tag{1.29}$$

$$K_p(t) = e_y(t) r^T(t) \overline{T} \tag{1.30}$$

$$\dot{K}_I(t) = e_y(t) r^T(t) T \tag{1.31}$$

$$K_I(0) = K_{I0} \tag{1.32}$$

$$e_y(t) = (y_m - y_p) \tag{1.33}$$

$$r^T(t) = \{e_y^T(t), x_m^T(t), u_m^T(t)\} \tag{1.34}$$

where T, $\overline{T}$ are time invariant weighting matrices, K_{I0} is the initial integral gain, and C_p is the time invariant plant output matrix.

It is shown in [12] that the tracking error is asymptotically stable provided that the plant can be stabilized using a constant output feedback gain $\tilde{K}_e$ and the stabilized closed loop transfer function matrix $H_{cl}(s) = C_p(sI - A_p + B_p\tilde{K}_eC_p)^{-1}B_p$ is strictly positive real (SPR). This special class of stabilizable minimum phase plants is defined as almost strictly positive real (ASPR).

1.2.3.2 Extension Using Parallel Feedforward

The algorithm of Section 1.2.3 requires the satisfaction of an ASPR condition on the plant. Therefore, parallel feedforward compensation was proposed to relax these constraints. Furthermore, the plant will not be required to be minimum phase.

Define $R_p(s)$ as a feedforward compensator with realization:

$$\dot{s_p}(t) = A_s s_p(t) + B_s u_p(t) \tag{1.35}$$

$$r_p(t) = D_p s_p(t) \tag{1.36}$$

The augmented output to be controlled is then

$$z_p(t) = y_p(t) + r_p(t) \tag{1.37}$$

and the augmented plant is

$$G_a(s) = G_p(s) + R_p(s) \tag{1.38}$$

The augmented tracking error will be

$$e_y^a(t) = y_m(t) - z_p(t) = y_m(t) - y_p(t) - D_p s_p(t) \tag{1.39}$$

and the adaptive algorithm becomes

$$K_r(t) = K_p(t) + K_I(t) \tag{1.40}$$

$$K_p(t) = e_y^a(t) r^T(t) \overline{T} \tag{1.41}$$

$$\dot{K}_I(t) = e_y^a(t) r^T(t) T \tag{1.42}$$

$$r^T(t) = [(e_y^a)^T(t), x_m^T(t), u_m^T(t)] \tag{1.43}$$

1.3 Contributions of the Thesis

1. A new result is obtained for eigenstructure invariance when it is known which control surface is most likely to fail. A basis for the subspace in which the eigenvectors of the failed system must lie is derived. We show mathematically, that if the j^{th} control surface will fail, then the j^{th} row of the constant output feedback gain matrix will be simply zero.

2. We obtain a passive fault tolerant flight controller for a control surface failure when it is not known in advance which surface will fail. An off-line multiobjective optimization technique to design an optimal control for a predefined class of control surface failures is proposed. We show that the time responses for the unfailed aircraft using the eigenstructure assignment gain and the fault tolerant gain are identical. Furthermore, the fault tolerant gain achieves MIL-F-8785C specifications for all failure conditions.

3. A new result is obtained for direct adaptive control of multi-input multi-output systems with control surface failures. The plant is aug-

mented with feedforward dynamics such that the inverse feedforward dynamics stabilizes the plant over the set of allowable failures. We prove that the augmented output error is asymptotically vanishing for loss of control effectiveness failures.

4. A novel state space approach for computing the feedforward around the plant is proposed. We use the MATLAB® LMI Toolbox [14] and the MATLAB® Optimization Toolbox [15] to find a feedback gain K which (1) stabilizes the plant for all possible failure configurations and (2) minimizes the inverse of the gain K. Then, the feedforward gain K^{-1} achieves the ASPR condition for all failure configurations.

5. Design of flight control laws for the linearized lateral dynamics of the F/A-18 aircraft using our new multiobjective optimization and adaptive methods.

1.4 Outline

Chapter 2 presents a new result for eigenstructure invariance when it is known which control surface is most likely to fail. The result is applied to a stability augmentation system for the linearized lateral dynamics of the F/A-18 aircraft.

Chapter 3 presents a passive fault tolerant flight control law for the F/A-18 aircraft which achieves acceptable handling qualities for a class of control surface failures.

Chapter 4 shows an alternative approach to the aircraft flight control surface failure problem. This approach uses direct model reference adaptive control to adjust the controller gains in real time to maintain stability when a failure occurs. A novel state space approach for computing the feedforward is described. The use of our algorithm is demonstrated by application to a three input model of the linearized lateral dynamics of the F/A-18 aircraft.

Chapter 2

Eigenstructure Invariance For An Anticipated Flight Control Surface Failure

2.1 Overview

In this chapter, we obtain a new result for eigenstructure invariance when it is known in advance which control surface is most likely to fail. We seek a constant gain output feedback controller such that the dominant eigenstructure is invariant under this failure.

2.2 Problem Statement

Consider the linearized lateral dynamics of an aircraft described by

$$\dot{x} = Ax + Bu \tag{2.1}$$

$$y = Cx \tag{2.2}$$

where $x \in \Re^n$ is the state vector, $u \in \Re^m$ is the input vector, $y \in \Re^r$ is the output vector, and A, B, C are matrices of appropriate dimensions.

The states are augmented with first order actuator dynamics and a yaw rate washout filter. Therefore, A, B, and C can be described by

$$A = \begin{bmatrix} -\delta I_m & 0_{m\times(n-m)} \\ A_{21} & A_{22} \end{bmatrix} \tag{2.3}$$

$$B = \delta \begin{bmatrix} I_m \\ 0_{(n-m)\times m} \end{bmatrix} \tag{2.4}$$

$$C = \begin{bmatrix} 0_{r\times m} & (C_{12})_{r\times(n-m)} \end{bmatrix} \tag{2.5}$$

where A_{21} is the control derivative matrix, A_{22} is the stability derivative matrix, and the submatrices $-\delta I_m$ and δI_m together represent the first order actuator dynamics. Here I_m is the identity matrix and δ is the location of the poles of the actuators.

Suppose that the aircraft is subject to a control surface failure which is modeled by setting the corresponding column of the control derivative matrix A_{21} to zero. Each failure condition corresponds to one control surface being stuck at its trim value.

The aircraft, with a failure in the j^{th} control surface, may be described by

$$\dot{x} = A_f x + Bu \tag{2.6}$$

$$y = Cx \tag{2.7}$$

where

$$A_f = A + \Delta A \tag{2.8}$$

$$\Delta A = \begin{bmatrix} 0_m & 0_{m\times(n-m)} \\ -\Delta A_{21} & 0_{(n-m)\times(n-m)} \end{bmatrix} \tag{2.9}$$

$$\Delta A_{21} = \begin{bmatrix} 0 & \cdots & a_{(m+1)j} & \cdots & 0 \\ \vdots & \cdots & \vdots & \cdots & \vdots \\ 0 & \cdots & a_{nj} & \cdots & 0 \end{bmatrix} \tag{2.10}$$

where $\begin{bmatrix} a_{(m+1)j} \\ \vdots \\ a_{nj} \end{bmatrix}$ is the j^{th} column of the control derivative matrix A_{21}.

2.3 Eigenstructure Invariance Main Result

Suppose we know which control surface is most likely to fail. We seek a constant gain output feedback controller such that the dominant eigenstructure is invariant under this failure. We will show mathematically that the solution is that the surface which will fail should not be used. That is, if the j^{th} control surface will fail, then the j^{th} row of the constant output feedback gain matrix will be zero. We present some interesting intermediate results. First we derive a basis for the subspace in which the eigenvectors of the failed aircraft must lie. Then, we show that a constant output feedback gain matrix exists which yields an invariant dominant eigenstructure both before and after failure. Finally, we show that the j^{th} row of this feedback gain matrix will be zero.

2.3.1 Eigenstructure Invariance

The following lemma derives a basis for the subspace in which the eigenvectors of the failed aircraft must lie.

Lemma 2.1 *Let λ_i^d, $i = 1, 2, \ldots, r$ be the set of desired eigenvalues. A basis for the m-dimensional subspace spanned by the columns of*

$(\lambda_i^d I - A_f)^{-1}B$ *is given by*

$$\left[\begin{array}{c}\alpha_1\delta\\0\\\vdots\\0\\\hline\gamma_1\end{array}\right],\ldots,\left[\begin{array}{c}0\\\vdots\\0\\\alpha_j\delta\\0\\\vdots\\0\\\hline\gamma_j\end{array}\right],\ldots,\left[\begin{array}{c}0\\\vdots\\0\\\alpha_m\delta\\\hline\gamma_m\end{array}\right] \tag{2.11}$$

where

$$\alpha_k = \frac{(\lambda_i^d+\delta)\delta det(A_{kk}^i)}{det(A^i)}; k = 1,\ldots,m. \tag{2.12}$$

$$\gamma = \left[\gamma_1,\ldots,\gamma_m\right] = \delta(Adj(A^i))_{21} \tag{2.13}$$

$$A^i = (\lambda_i^d I - A_f) \tag{2.14}$$

$$Adj(A^i) = \left[\begin{array}{cc}(\lambda_i^d+\delta)\Gamma & (Adj(A^i))_{12}\\(Adj(A^i))_{21} & (Adj(A^i))_{22}\end{array}\right] \tag{2.15}$$

and where $\Gamma = diag\{det(A_{11}^i),\ldots,det(A_{kk}^i),\ldots,det(A_{mm}^i)\}$

Proof of Lemma 2.1: See Appendix A

The following theorem is an existence theorem. It shows the existence of a

constant output feedback gain matrix F which yields an invariant dominant eigenstructure both before and after failure.

Theorem 2.1 *There exists a constant output feedback controller* $u = Fy$ *such that:*

$$(A_f + BFC)v_i^f = (A + BFC)v_i^f = \lambda_i^d v_i^f;\ i = 1,2,\ldots,r \tag{2.16}$$

Proof of Theorem 2.1: See Appendix B

The following theorem shows that the failure of the j^{th} control surface causes the j^{th} row of the constant output feedback gain matrix F to be zero.

Theorem 2.2 *The constant feedback gain F from Theorem 2.1 has all zeros in row j.*

Proof of Theorem 2.2: See Appendix C

2.4 Example

We consider the linearized lateral dynamics of the F/A-18A aircraft. The rigid body states are lateral(side) velocity(v), yaw rate (r), roll rate (p), and bank angle (ϕ). These states are augmented with first order actuator dynamics and a yaw rate washout filter to yield a 9^{th} order model. The control surfaces are asymmetric stabilator (δ_{sc}), asymmetric trailing edge flaps (δ_{tec}), ailerons (δ_{ac}), and rudder (δ_{rc}). The inputs are stabilator command (δ_{sc}), trailing edge flaps command (δ_{tec}), ailerons command (δ_{ac}), and rudder command (δ_{rc}). The measurements are sideslip angle (β), washed out yaw rate (r_{wo}), and roll rate (p). A control surface failure is modeled by setting the corresponding column in the control derivative matrix A_{21} to zero. Each failure condition corresponds to one control surface being stuck at its trim value. The state space matrices A, B, and C are shown below:

$$A = \begin{bmatrix} -30 & 0 & 0 & 0 & 0 & 0 & 0 & 0 & 0 \\ 0 & -30 & 0 & 0 & 0 & 0 & 0 & 0 & 0 \\ 0 & 0 & -30 & 0 & 0 & 0 & 0 & 0 & 0 \\ 0 & 0 & 0 & -30 & 0 & 0 & 0 & 0 & 0 \\ -6.93 & 0 & -2.915 & 34.909 & -0.245 & -646.9 & 0.0285 & 32.189 & 0 \\ -0.396 & -0.835 & -0.896 & -3.26 & 0.00849 & -0.2460 & 0.112 & 0 & 0 \\ 11.86 & 13.06 & 13.14 & 4.4 & -0.0256 & 0.73 & -2.83 & 0 & 0 \\ 0 & 0 & 0 & 0 & 0 & 0 & 1 & 0 & 0 \\ 0 & 0 & 0 & 0 & 0 & 0.5 & 0 & 0 & -0.5 \end{bmatrix} \quad (2.17)$$

$$B^T = \begin{bmatrix} 30 & 0 & 0 & 0 & 0 & 0 & 0 & 0 & 0 \\ 0 & 30 & 0 & 0 & 0 & 0 & 0 & 0 & 0 \\ 0 & 0 & 30 & 0 & 0 & 0 & 0 & 0 & 0 \\ 0 & 0 & 0 & 30 & 0 & 0 & 0 & 0 & 0 \end{bmatrix} \quad (2.18)$$

$$C = \begin{bmatrix} 0 & 0 & 0 & 0 & 1/650 & 0 & 0 & 0 & 0 \\ 0 & 0 & 0 & 0 & 0 & 1 & 0 & 0 & -1 \\ 0 & 0 & 0 & 0 & 0 & 0 & 1 & 0 & 0 \end{bmatrix} \quad (2.19)$$

We consider a rudder failure which is modeled by setting the 4^{th} column of the control derivative matrix A_{21} to zero.

First, we design an eigenstructure assignment controller for the unfailed

condition by assigning the dutch roll mode to have a damping of 0.707 and a natural frequency of 2.83 r/s. The roll subsidence mode is assigned to its open loop value of -2.76. The desired dutch roll eigenvectors are chosen for a sideslip and yaw rate mode which is decoupled from the roll rate and bank angle. The desired roll subsidence eigenvector is chosen for a roll rate mode which is decoupled from lateral velocity and yaw rate. The achievable eigenvectors can be computed using the orthogonal projection of the i^{th} desired eigenvector v_i^d onto the subspace spanned by the columns of $L_i = (\lambda_i I - A)^{-1}B$ as suggested by Andry et. al. [17]. An alternative representation is described by Kautsky et. al. [21], who showed that the subspace in which the eigenvector v_i must reside is also given by the null space of $U_1^T(\lambda_i I - A)$. The matrix U_1 is obtained from the singular value decomposition of B, which is given by

$$B = \begin{bmatrix} U_0 & U_1 \end{bmatrix} \begin{bmatrix} \Sigma V^T \\ 0 \end{bmatrix} \tag{2.20}$$

The method of Kautsky et. al. [21] is the preferred method for numerical computation of subspaces and it is used to compute the achievable eigenvectors in our example.

The output feedback gain matrix using eigenstructure assignment is shown

by Andry et. al. [17] to be

$$F = -(Z - A_1 V)(CV)^{-1} \tag{2.21}$$

where A_1 is a partition of the matrix A in (2.1), V is the matrix whose columns are the r achievable eigenvectors, Z is a matrix whose columns are related to the r achievable eigenvalues and eigenvectors, and C is the output matrix in (2.2). An alternative representation for the feedback gain matrix F is shown by Sobel et. al. [22] to be

$$F = -V_b \Sigma_b^{-1} U_{b0}^T (V\Lambda - AV) V_r \Sigma_r^{-1} U_{r0}^T \tag{2.22}$$

where the singular value decomposition of the matrices B and CV are given by

$$B = \begin{bmatrix} U_{b0} & U_{b1} \end{bmatrix} \begin{bmatrix} \Sigma_b V_b^T \\ 0 \end{bmatrix} \tag{2.23}$$

$$CV = \begin{bmatrix} U_{r0} & U_{r1} \end{bmatrix} \begin{bmatrix} \Sigma_r V_r^T \\ 0 \end{bmatrix} \tag{2.24}$$

and where Λ is an $r \times r$ diagonal matrix with entries λ_i, $i = 1, 2, \ldots, r$. The method described by (2.22) is the preferred method for numerical computation and is used for the design of our eigenstructure assignment controller for the unfailed condition.

The eigenstructure assignment output feedback matrix computed for the unfailed aircraft is shown in Table 2.1. The time responses of sideslip angle, yaw rate, roll rate, and bank angle to a one degree initial sideslip using the eigenstructure assignment gain computed for the no failure condition are shown in Figure 2.1. Observe the degradation in the time responses after failure.

Table 2.1: Gain matrix computed for no failure

β	r_{wo}	p	
0.2412	0.0562	-0.0009	δ_{sc}
0.1317	0.1742	0.0038	δ_{tec}
0.1352	0.1918	0.0047	δ_{ac}
-0.8366	0.9019	0.0379	δ_{rc}

Next, we compute an optimal feedback gain using Theorem 2.2 by imposing simultaneous specifications on the unfailed and rudder failure conditions. We require the dutch roll and roll modes for both the unfailed and failed conditions to be the same as for the eigenstructure assignment controller. Furthermore, we require that the fourth row of the dutch roll and roll eigenvectors be zero for both the unfailed and failed conditions.

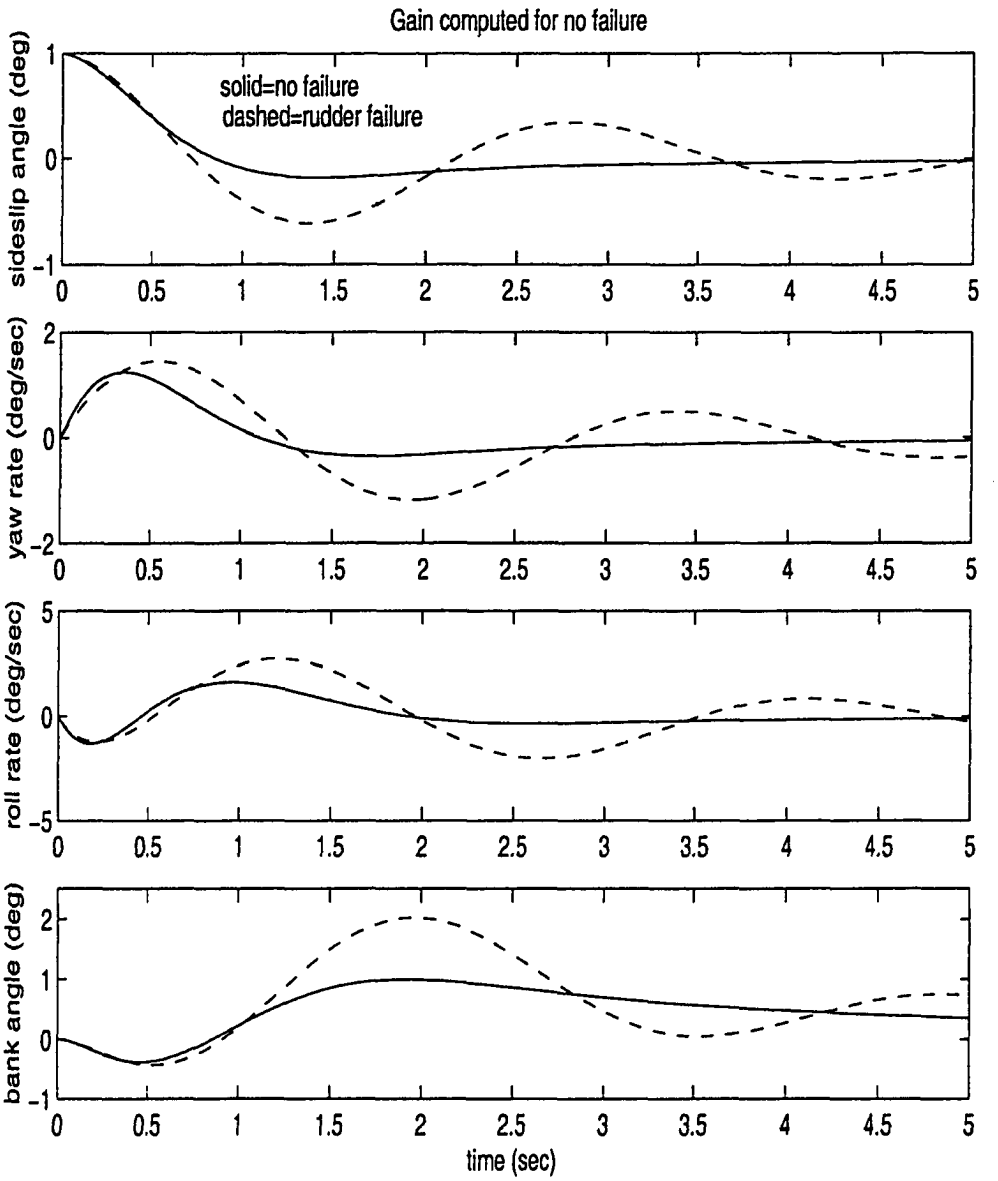

Figure 2.1: Gain computed for no failure

The parameter vector contains the quantities which may be varied by the optimization. This vector includes $Re(\lambda_{dr})$, $Im(\lambda_{dr})$, λ_{roll}, z_1, and z_3. Here, the vectors z_i contain the free eigenvector parameters. That is, the i^{th} eigenvector v_i may be written as

$$v_i = L_i z_i \tag{2.25}$$

where the columns of $L_i = (\lambda_i I - A)^{-1} B$ are the basis for the subspace in which the i^{th} eigenvector must reside. Thus, the free parameters are the vectors z_i rather than the eigenvectors v_i.

The optimization is performed by using the multiobjective optimization method which is implemented in the MATLAB® Optimization Toolbox [15] program ATTGOAL. The optimization is initialized with the eigenstructure assignment controller and the free parameters of the unfailed condition.

The output feedback gain matrix is shown in Table 2.2. Observe that the fourth row of this gain matrix is exactly zero. The initial condition responses using the optimal gain are shown in Figure 2.2. Observe that the eigenstructure invariance is achieved but with increased coupling from sideslip to roll rate and bank angle. To reduce the coupling, the number of eigenvector ob-

jectives is reduced by only requiring the fourth row of the dutch roll eigenvector to be zero. The feedback gain matrix is shown in Table 2.3 where we observe that the gains in the fourth row are small but nonzero.

Table 2.2: Gain using theorem 2.2 (dutch roll and roll modes)

β	r_{wo}	p	
-9.1724	-5.6198	-0.2616	δ_{sc}
4.7829	4.8542	0.1423	δ_{tec}
-13.0675	5.2913	0.2041	δ_{ac}
0	0	0	δ_{rc}

Table 2.3: Gain using theorem 2.2 (dutch roll only)

β	r_{wo}	p	
8.2678	-7.6184	-0.1597	δ_{sc}
-4.0159	2.7116	0.0564	δ_{tec}
-3.9988	4.5213	0.0944	δ_{ac}
0.0613	0.0298	0.0198	δ_{rc}

The initial condition responses using this optimal gain are shown in Figure 2.3. We observe that the coupling from sideslip to roll rate and bank angle

has been significantly reduced, albeit at the expense of exact eigenstructure invariance.

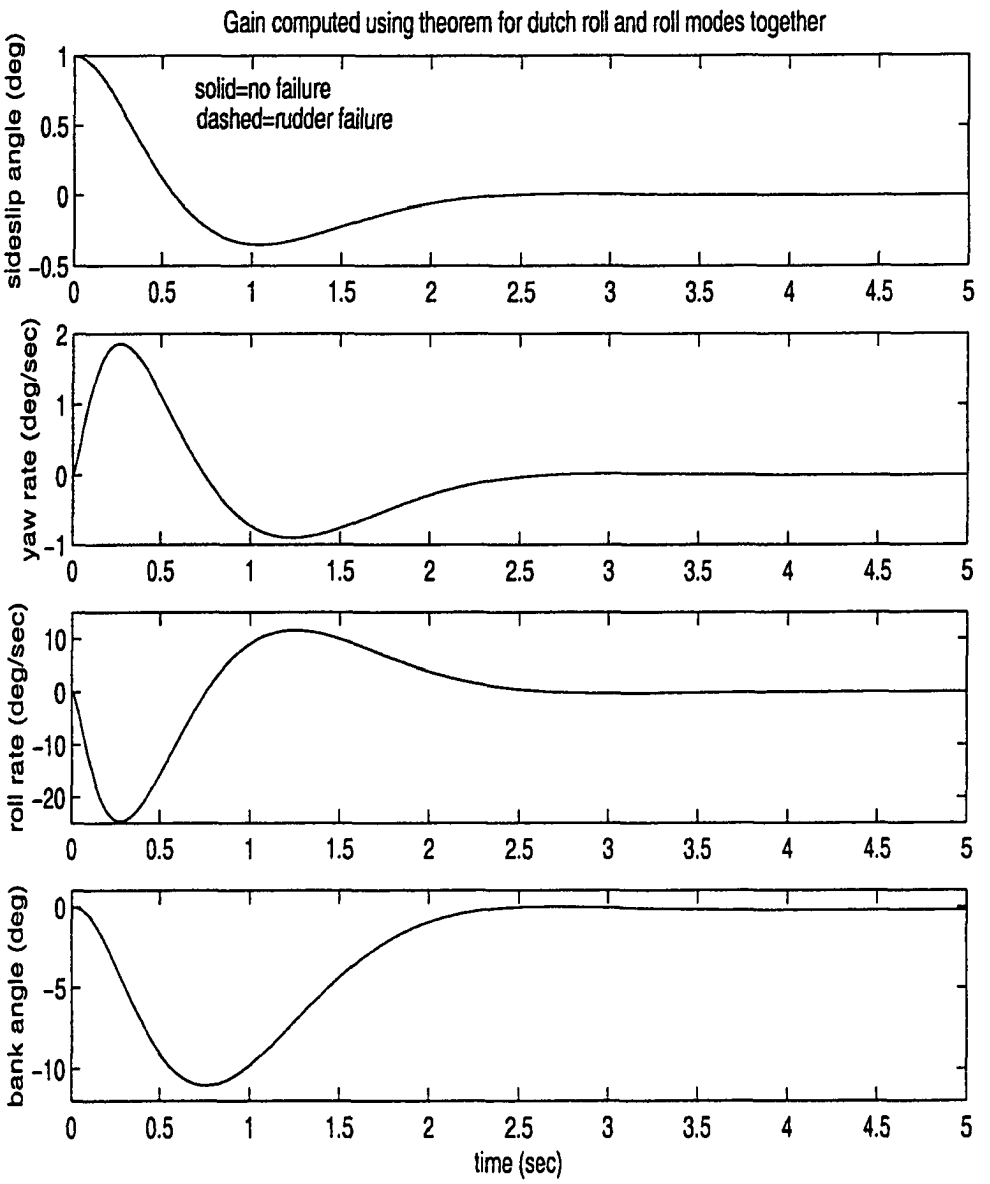

Figure 2.2: Gain computed using theorem 2.2 for dutch roll and roll

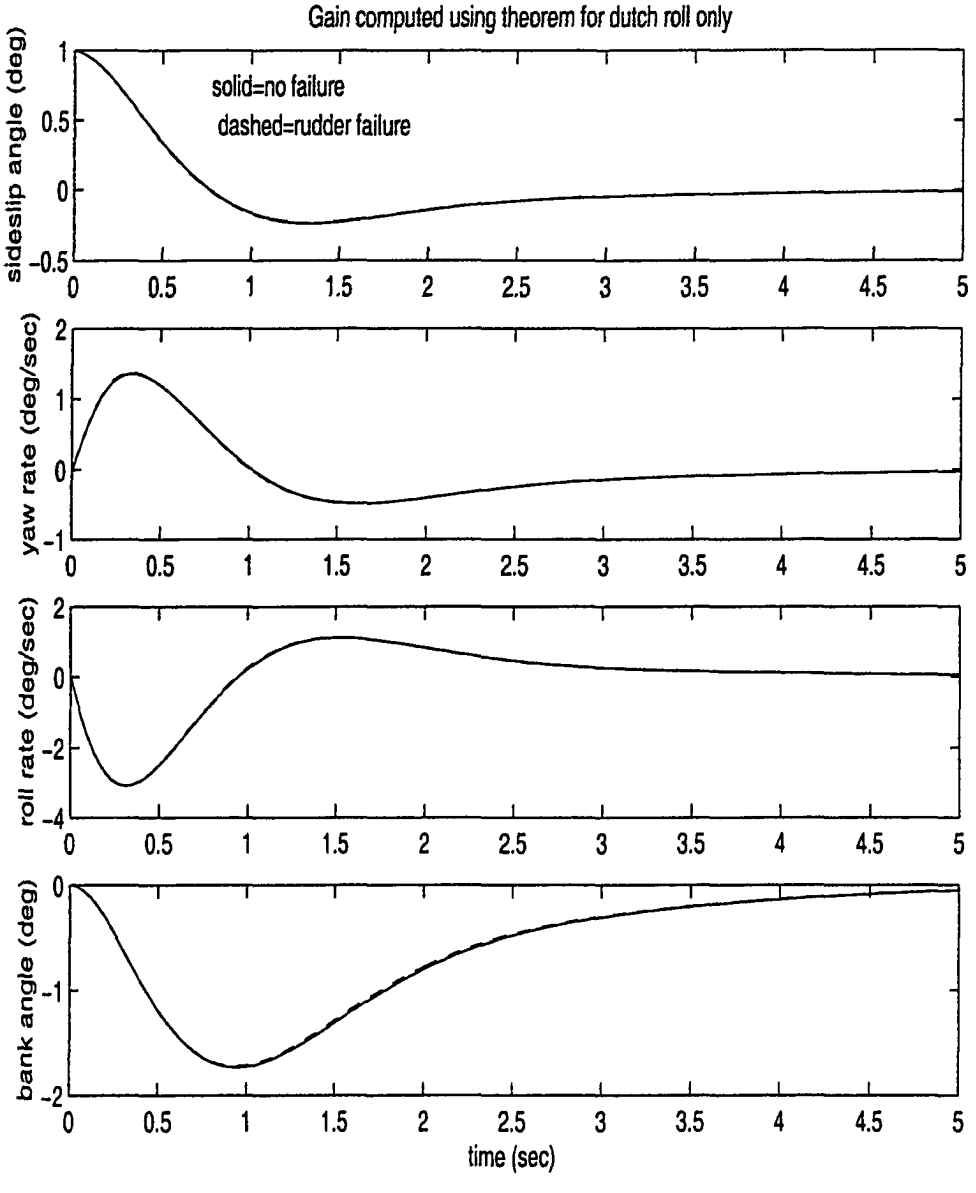

Figure 2.3: Gain computed using theorem 2.2 for dutch roll mode

Chapter 3

Passive Fault Tolerant Control for an Unknown Control Surface Failure

3.1 Overview

In this chapter, we design an optimal gain which is tolerant to a control surface failure. The class of control surface failures we consider includes the symmetric failure of any one control surface with the surface being stuck at its trim value. It is not known in advance which surface will fail. We compare an eigenstructure assignment gain designed for the unfailed aircraft

with a multiobjective optimization gain designed to achieve (1) the same response for the unfailed condition as was obtained using eigenstructure assignment and (2) MIL-F-8785C specifications for all failure conditions belonging to our class.

3.2 Problem Formulation

Consider the linearized lateral dynamics of an aircraft described by

$$\dot{x} = Ax + Bu \tag{3.1}$$

$$y = Cx \tag{3.2}$$

where $x \in \Re^n$ is the state vector, $u \in \Re^m$ is the input vector, $y \in \Re^r$ is the output vector, and A, B, C are described by Eqs. (2.3)-(2.5).

Suppose that the plant is subject to a control surface failure. The class of control surface failures we consider includes the symmetric failure of any one control surface with the surface being stuck at its trim value. However, it is not known in advance which control surface will fail.

The aircraft, with a failure in the j^{th} control surface, may be described by

$$\dot{x} = A_f x + Bu \tag{3.3}$$

$$y = Cx \tag{3.4}$$

where A_f is given by Eqs. (2.8)-(2.10).

We want to design an optimal controller which is tolerant to a control surface failure. Furthermore, this optimal controller should achieve (1) the same response for the unfailed condition as was obtained using eigenstructure assignment and (2) MIL-F-8785C specifications for all failure conditions belonging to our class.

3.3 Main Result

We propose an approach which uses off-line multiobjective optimization to design an optimal gain which is tolerant to a control surface failure. We use program ATTGOAL from the MATLAB® Optimization Toolbox [15] to solve the multiobjective goal attainment problem described by

$$\underset{x,\gamma}{\text{minimize}}\ \gamma \quad \text{s.t.} \quad F(x) - w\gamma \leq \text{GOAL}$$

where $F(x)$, w, and GOAL are given.

The function $F(x)$ is the objective function to be minimized at the point x. ATTGOAL attempts to minimize the function to attain the goal values given by GOAL. Alternatively, to make the objective function as near as possible to a goal value, the parameter OPTIONS(15) in ATTGOAL is set equal to

the number of objectives required to be in the neighborhood of goal values. These objectives must be partitioned into the first elements of the function $F(x)$. GOAL is a vector of values that the objectives attempt to attain. The weighting vector w is used to control the relative under-attainment or over-attainment of the objectives. The weighting function may be set equal to $w = \text{abs(GOAL)}$ to obtain the same percentage of under or over-attainment. When w is positive, ATTGOAL attempts to make the objectives less than the goal values. To make the objective functions greater than the goal values, w is set to be negative.

3.4 Example

We consider the linearized lateral dynamics of the F/A-18A aircraft which was described in Section 2.4. A control surface failure is modeled by setting the corresponding column of the control derivative matrix A_{21} to zero.

First, we design an eigenstructure assignment controller for the unfailed condition by assigning the dutch roll mode to have a damping of 0.707 and a natural frequency of 2.83 r/s. The roll subsidence mode is assigned to its open loop value of -2.76. The desired dutch roll eigenvectors are cho-

sen for a sideslip and yaw rate mode which is decoupled from the roll rate and bank angle. The desired roll subsidence eigenvector is chosen for a roll rate mode which is decoupled from lateral velocity and yaw rate. The achievable eigenvectors can be computed using the orthogonal projection of the i^{th} desired eigenvector v_i^d onto the subspace spanned by the columns of $L_i = (\lambda_i I - A)^{-1}B$ as suggested by Andry et. al. [17]. An alternative representation is described by Kautsky et. al [21], who showed that the subspace in which the eigenvector v_i must reside is also given by the null space of $U_1^T(\lambda_i I - A)$. The matrix U_1 is obtained from the singular value decomposition of B, which is given by

$$B = \begin{bmatrix} U_0 & U_1 \end{bmatrix} \begin{bmatrix} \Sigma V^T \\ 0 \end{bmatrix} \tag{3.5}$$

The method of Kautsky et. al. [21] is the preferred method for numerical computation of subspaces and it is used to compute the achievable eigenvectors in our example.

The output feedback gain matrix using eigenstructure assignment is shown by Andry et. al. [17] to be

$$F = -(Z - A_1 V)(CV)^{-1} \tag{3.6}$$

where A_1 is a partition of the matrix A in (3.1), V is the matrix whose columns are the r achievable eigenvectors, Z is a matrix whose columns are related to the r achievable eigenvalues and eigenvectors, and C is the output matrix in (3.2). An alternative representation for the feedback gain matrix F is shown by Sobel et. al. [22] to be

$$F = -V_b \Sigma_b^{-1} U_{b0}^T (V\Lambda - AV) V_r \Sigma_r^{-1} U_{r0}^T \tag{3.7}$$

where the singular value decomposition of the matrices B and CV are given by

$$B = \begin{bmatrix} U_{b0} & U_{b1} \end{bmatrix} \begin{bmatrix} \Sigma_b V_b^T \\ 0 \end{bmatrix} \tag{3.8}$$

$$CV = \begin{bmatrix} U_{r0} & U_{r1} \end{bmatrix} \begin{bmatrix} \Sigma_r V_r^T \\ 0 \end{bmatrix} \tag{3.9}$$

and where Λ is an $r \times r$ diagonal matrix with entries λ_i, $i = 1, 2, \ldots, r$. The method described by (3.7) is the preferred method for numerical computation and is used for the design of our eigenstructure assignment controller for the unfailed condition.

Table 3.1 shows the desired dutch roll and roll subsidence eigenvectors, the eigenvectors from the projections onto the achievable subspaces, and the eigenvectors of $(A + BFC)$ where F is the eigenstructure assignment output feedback gain matrix.

Table 3.1: Desired and Achievable Eigenvectors (actuator entries not shown)

Desired		Projection		$(A+BFC)$		
Dutch Roll	Roll	Dutch Roll	Roll	Dutch Roll	Roll	
$1+jx$	0	$1+j0$	0.0001	$1-j59.4$	0.0001	v
$x+j1$	0	$0.0028+j1$	-0.0168	$0.0032+j1$	-0.0168	r
$0+j0$	1	$-0.0137+j3.83$	1	$-0.012+j5.24$	1	p
$0+j0$	x	$0.0006+j2.14$	-0.362	$-0.0003-j2.52$	-0.362	ϕ
$x+jx$	0	$-0.0008+j0.034$	0.0037	$-0.0008+j0.08$	0.0037	x_9

First, from Table 3.1, we remark that the entries in the imaginary part of the dutch roll eigenvectors, which we desire to be zero, are not zero after projecting onto the achievable subspace. This will cause coupling to the roll rate response. The reason that we do not achieve the zero eigenvector entries is that the $\tilde{L}_i$ are poorly conditioned. So to achieve a gain matrix with reasonable magnitude, we discard the smallest singular value when computing the pseudo inverse to obtain z_i. If less coupling is required then another choice for the desired dutch roll eigenvectors should be made which specifies fewer entries. Second, we remark that we have $r < m$ (i.e. the number of outputs is less than the number of inputs) which is different from most aerospace applications of eigenstructure assignment which have appeared

in the literature. Some authors have suggested assigning the left eigenvectors when $r < m$. However, the right eigenvectors still lie in the subspaces spanned by the columns of $(\lambda_i I - A)^{-1}B$. Since we only assign r eigenvalues, we can also assign m entries in the corresponding eigenvectors. This is independent of the relation between r and m. The eigenstructure assignment feedback gain matrix is shown in Table3.2.

Table 3.2: Eigenstructure Assignment Feedback Gain Matrix

β	r_{wo}	p	
0.2412	0.0562	-0.0009	δ_{sc}
0.1317	0.1742	0.0038	δ_{tec}
0.1352	0.1918	0.0047	δ_{ac}
-0.8366	0.9019	0.0379	δ_{rc}

The sideslip angle responses to a one degree initial sideslip for the unfailed and four failure conditions are shown in Figure 3.1 where the oscillatory response corresponds to a rudder failure. We remark that the response is unacceptable when a rudder failure occurs. In fact, the dutch roll damping is only $\zeta = 0.18$ when a rudder failure occurs. This is significantly less than the minimum value of $\zeta = 0.4$ which is required in MIL-F-8785C. We fur-

ther remark that the asymmetric stabilator, asymmetric trailing edge flaps, and ailerons are all good producers of rolling moment, but only rudder is a good producer of yawing moment. Thus, a rudder failure is the most difficult condition for achieving desirable handling qualities.

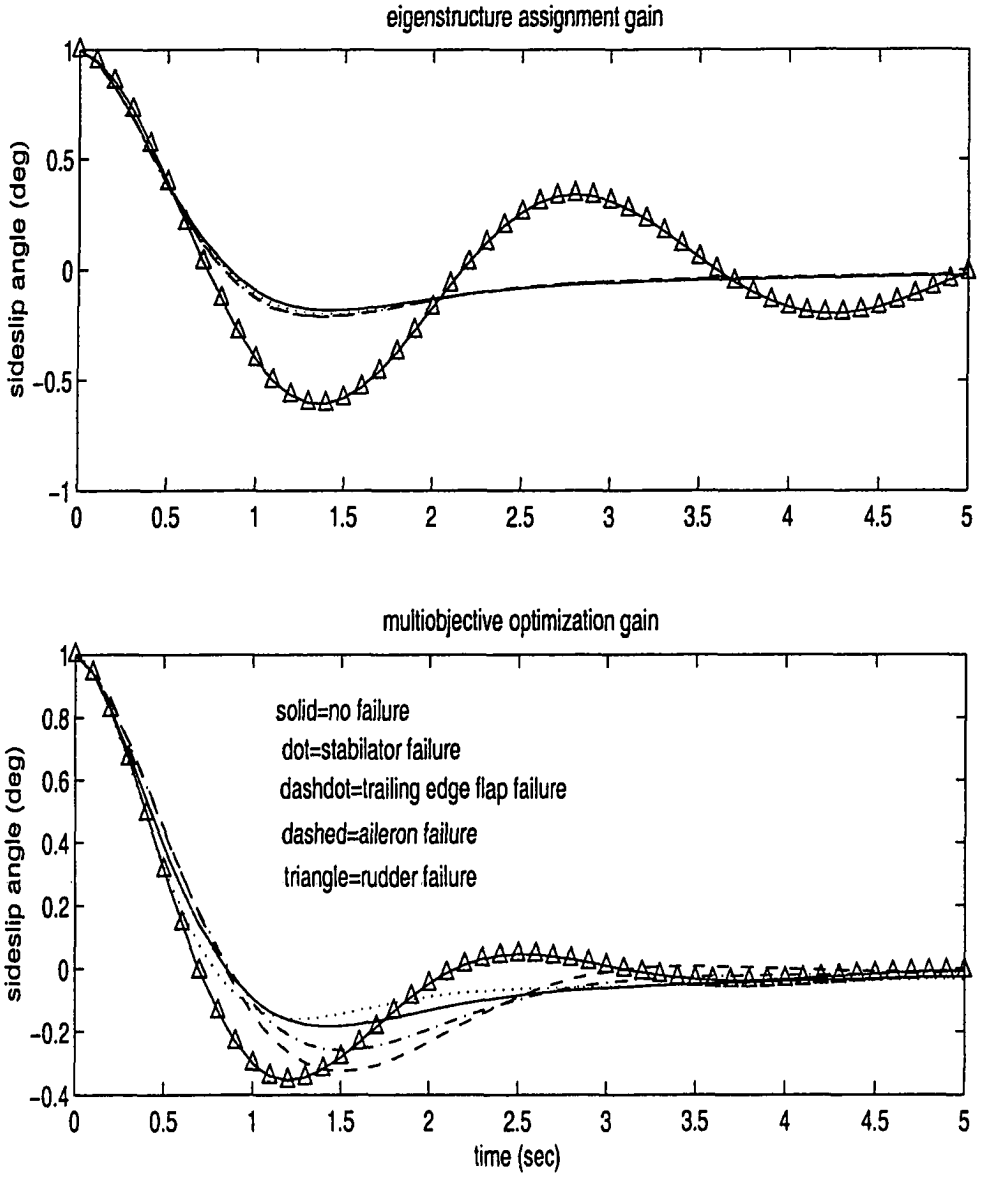

Figure 3.1: Sideslip angle responses

Next, we design an optimized controller by imposing simultaneous specifications on the unfailed and four failure conditions. We use the multi-objective optimization method which is implemented in the MATLAB® Optimization Toolbox [15] program ATTGOAL. Our objective is for the optimal unfailed responses to be the same as the eigenstructure assignment unfailed responses while also achieving MIL-F-8785C specifications for the failed responses. The MIL-F-8785C specifications for Level 1, Category A (CO and GA), Class IV flight are as follows: dutch roll damping and natural frequency greater than 0.4 and 1.0, respectively; roll subsidence time constant less than 1 second; and spiral time to double amplitude greater than 12 seconds. We remark that the eigenstructure assignment controller achieves all these specifications with the exception of the dutch roll damping which is 0.18 when a rudder failure occurs.

We compute an optimal feedback gain using the following objectives:
(1) the dutch roll and roll subsidence modes are to be the same as for the eigenstructure assignment controller, and (2) the dutch roll and roll subsidence modes are to achieve MIL-F-8785C specifications for the four failure conditions. We remark that we cannot directly specify the spiral mode when using a stability augmentation system (SAS) which does not feedback bank

angle.

The optimization parameters are (1) the real part of the dutch roll eigenvalue $\mathrm{Re}(\lambda_{dr})$, (2) the imaginary part of the dutch roll eigenvalue $\mathrm{Im}(\lambda_{dr})$, (3) the roll subsidence eigenvalue λ_{roll}, (4) the free eigenvector parameters z_{roll} for the roll subsidence mode, and (5) the free eigenvector parameters z_{dr} for the dutch roll mode where real arithmetic is used. Here, the vectors z_i contain the free parameters. That is, the i^{th} eigenvector v_i may be written as

$$v_i = L_i z_i \tag{3.10}$$

where the columns of $L_i = (\lambda_i I - A)^{-1} B$ are the basis for the subspace in which the i^{th} eigenvector must reside. Thus, the free parameters are the vectors z_i rather than the eigenvectors v_i. The parameters are initialized at the values obtained when using the eigenstructure assignment gain.

The objectives and weightings at the unfailed condition are

$$\lambda_{roll} = -2.76 \quad , \quad w = \mathrm{abs}(-2.76)$$

$$\mathrm{Re}(\lambda_{dr}) = -2 \quad , \quad w = \mathrm{abs}(-2)$$

$$\mathrm{Im}(\lambda_{dr}) = 2 \quad , \quad w = \mathrm{abs}(2)$$

The objectives and weightings at the 4 failure conditions are

$$\zeta_{\mathrm{dr}}^{i} \geq 0.4 \quad , \quad w^{i} = -1; \quad i = 1,\ldots,4$$

$$(\omega_n)_{\mathrm{dr}}^{i} \geq 1.0 \quad , \quad w^{i} = -1; \quad i = 1,\ldots,4$$

The optimal gain is shown in Table 3.3 which required 2.04 seconds of CPU time and 52 function evaluations. The sideslip angle response to a one degree initial sideslip is shown in Figure 3.1. We observe that all responses achieve the desired specifications. The dutch roll damping ζ_{dr} is now 0.4 for the rudder failure condition which achieves the MIL-F-8785C specification.

Table 3.3: Optimal Feedback Gain Matrix

β	r_{wo}	p	
5.2056	-2.851	-0.0605	δ_{sc}
-2.1993	1.4108	0.0292	δ_{tec}
-2.651	1.9134	0.0400	δ_{ac}
-0.0766	0.4808	0.0293	δ_{rc}

The yaw rate responses for an initial sideslip for the eigenstructure assignment and multiobjective optimization gains are shown in Figure 3.2. Again we observe that the eigenstructure assignment gain exhibits an unacceptable oscillation when a rudder failure occurs whereas the multiobjective optimization gain yields an acceptable response.

The roll rate responses for the eigenstructure assignment and multiobjective optimization gains are shown in Figure 3.3. Here we observe that the roll rate response with the multiobjective optimization gain exhibits a significant coupling from sideslip to roll rate when a stabilator failure occurs.

The bank angle responses for the eigenstructure assignment and multiobjective optimization gains are shown in Figure 3.4. Again, we observe that the response with the multiobjective optimization gain exhibits a significant coupling from sideslip to bank angle when a stabilator failure occurs. However, the MIL-F-8785C specification on sideslip to bank angle coupling is that the minimum $\zeta\omega_n$ is increased if $\omega_n^2|\phi/\beta| > 20$. For our aircraft with a stabilator failure we have $\omega_n^2|\phi/\beta| < (2.83)^2(2.2) = 17.6 < 20$. Therefore, our responses meet the MIL specification even though a smaller sideslip to bank angle coupling may be desirable.

The responses for the unfailed aircraft to an initial sideslip are shown in Figure 3.5 for both the eigenstructure assignment and multiobjective optimization gains. We observe that the sideslip and yaw rate responses are identical and there is only an insignificant degradation in the coupling from sideslip to roll rate. Figure 3.6 shows the responses using both gains for the unfailed aircraft until time $t = 0.5$ sec when a rudder failure occurs. We observe that the eigenstructure assignment gain allows oscillation and large settling time whereas the multiobjective optimization gain yields an acceptable response after failure.

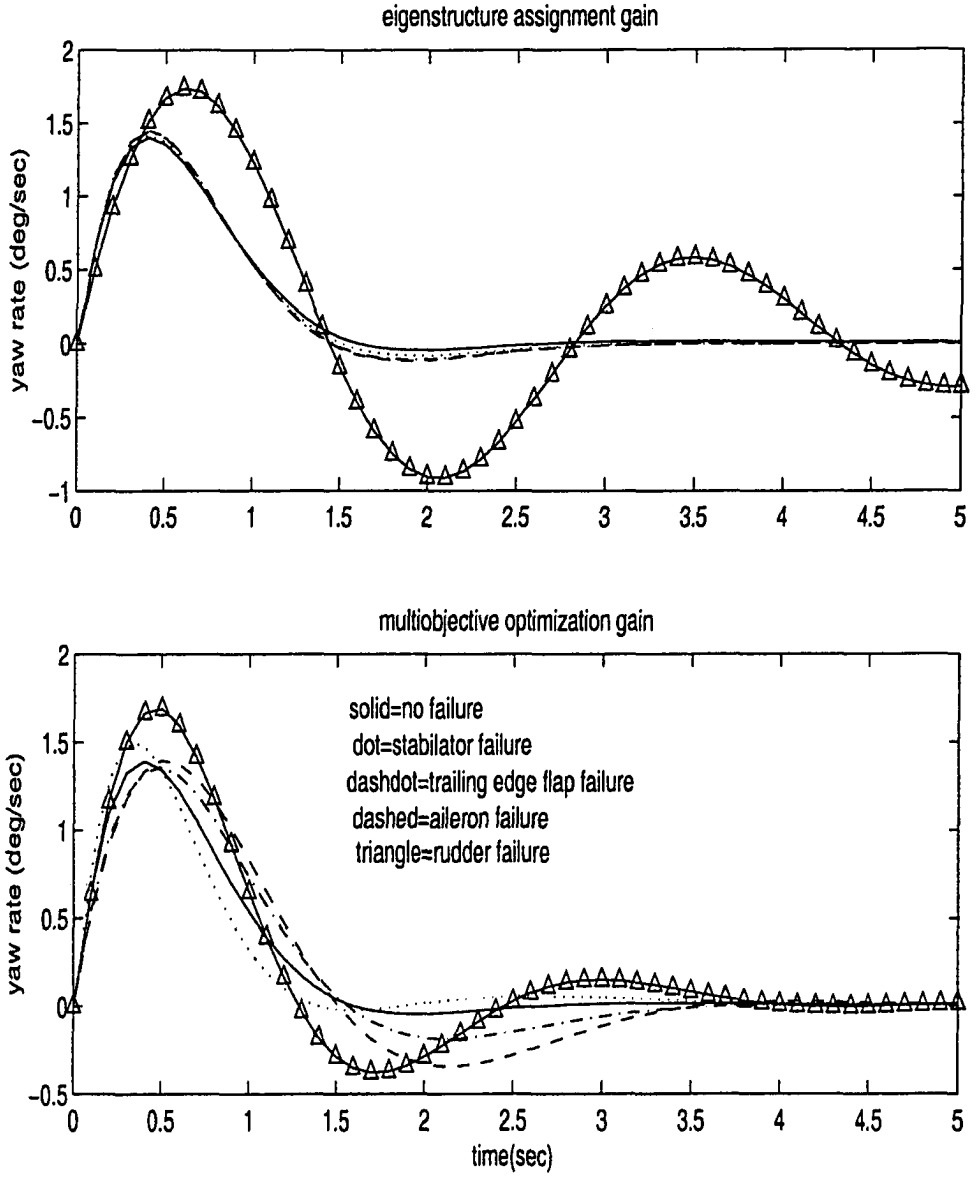

Figure 3.2: Yaw rate responses

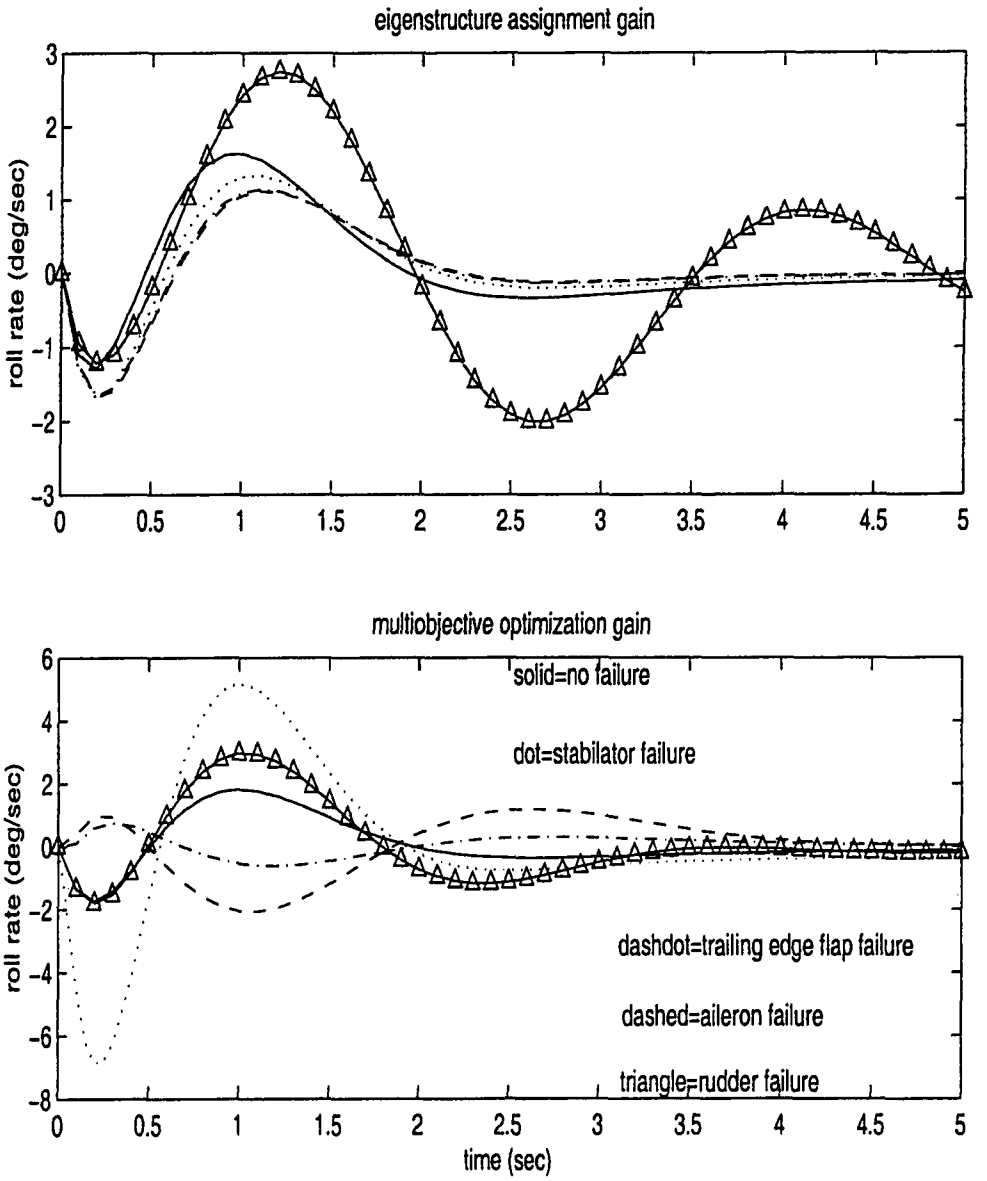

Figure 3.3: Roll rate responses

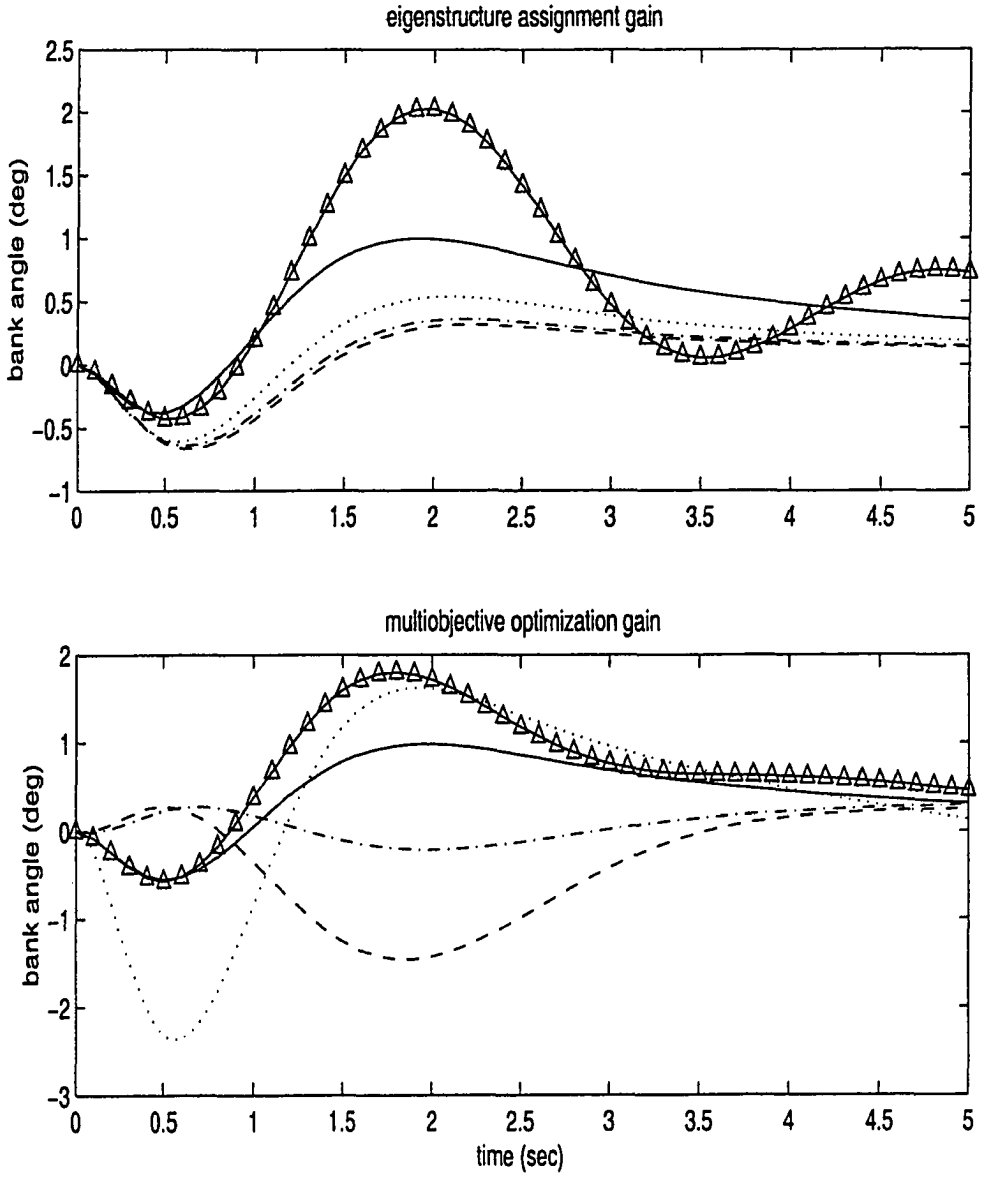

Figure 3.4: Bank angle responses

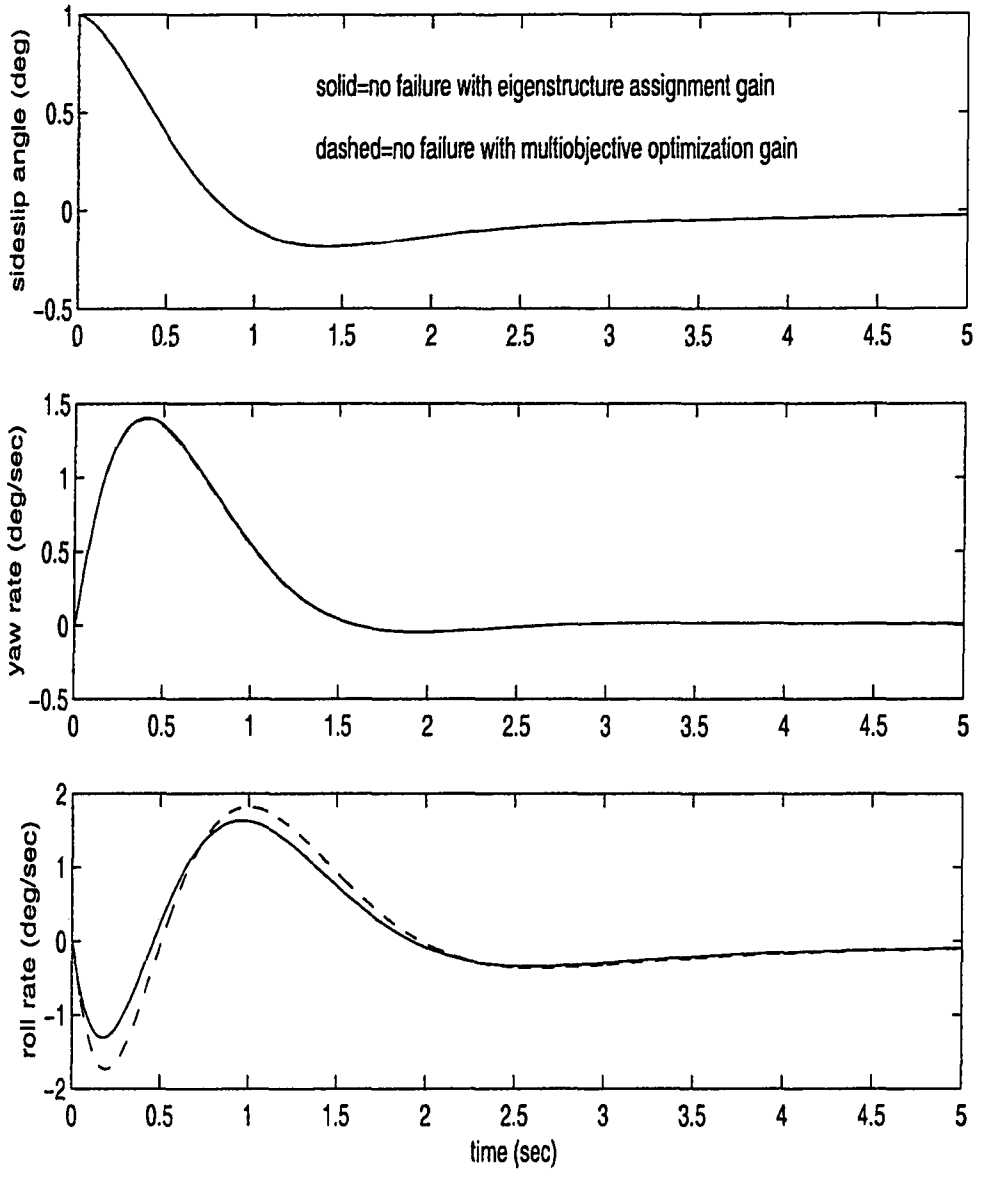

Figure 3.5: Responses for eigenstructure assignment gain and multiobjective optimization gain with no failure

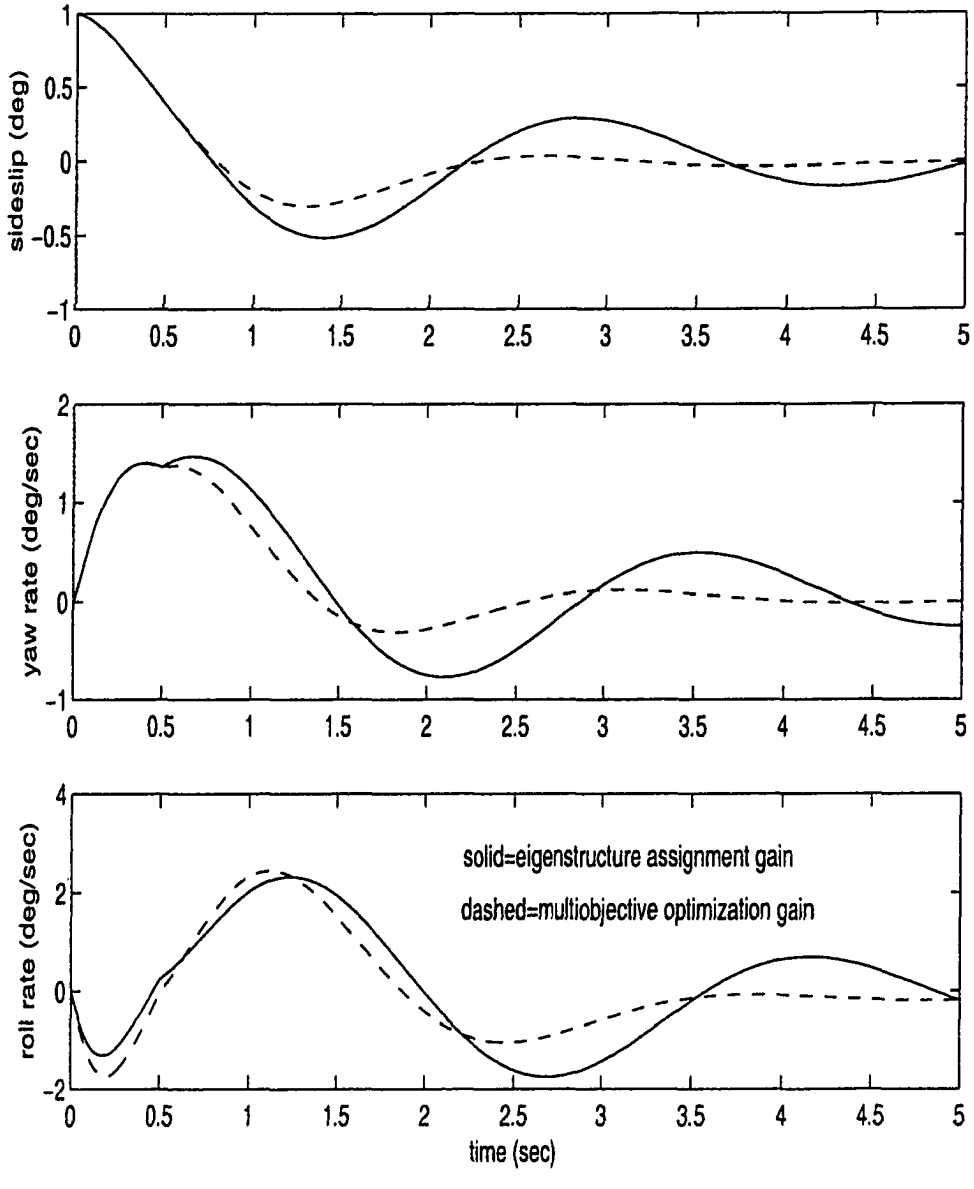

Figure 3.6: Responses for rudder failure at $t = 0.5$sec

Chapter 4

Adaptive Control in The Presence of Loss of Control Effectiveness

4.1 Overview

In this chapter, we extend a direct adaptive controller for multi-input multi-output plants which was proposed by Kaufman et. al. [12] to plants with loss of control effectiveness failures. An important property of direct adaptive control is that the control gains are computed directly without an explicit identification of the system parameters. Furthermore, the direct adaptive control algorithm in [12] is applicable to non minimum phase systems, and the order of the plant may be much larger than the order of the reference

model. In Ref. [12], stability is proven for plants that are almost strictly positive real (ASPR) for all possible plant parameter values. To achieve the ASPR condition, the authors insert a feedforward compensator around the plant so that the augmented system is ASPR.

We augment the plant with a feedforward compensator such that the inverse feedforward stabilizes the plant over the set of allowable failures. We prove that the augmented output error is asymptotically vanishing for a loss of control effectiveness failure. We propose a novel state space approach for computing the feedforward compensator. We use the MATLAB® LMI Toolbox [14] and and the MATLAB® Optimization Toolbox [15] to find a feedback gain K which (1) stabilizes the plant for all possible failure configurations and (2) minimizes the inverse of the gain K. Then, the plant augmented with the feedforward gain K^{-1} achieves the ASPR condition for all failure configurations.

We demonstrate the use of our algorithm by application to a three input model of the linearized lateral dynamics of the F/A-18 aircraft. Simulation results are presented which show that the adaptive controller exhibits improved model following as compared to a fixed gain eigenstructure as-

signment controller.

4.2 Problem Statement

Let (T_i, T_{i+1}), $i = 0, 1, \ldots, q_0$, with $T_0 = 0$, be the time intervals on which the control surface failure pattern is fixed. That is, control surfaces only fail at time T_i, $i = 1, \ldots, q_0$. Then, the plant on the interval (T_i, T_{i+1}), $i = 0, 1, \ldots, q_0$ is described by

$$\mathcal{P}_i : \begin{cases} \dot{x}_p(t) &= A_p x_p(t) + B_p^i u_p(t) \\ y_p(t) &= C_p x_p(t) \end{cases} \tag{4.1}$$

where $A_p \in \Re^{n_p \times n_p}$, $B_p \in \Re^{n_p \times m}$, $C_p \in \Re^{q \times n_p}$, $B_p^i = B_p \alpha^i$, and $B_p \equiv B_p^0$.

$$\alpha^i = \begin{cases} diag\{\alpha_1^i, \alpha_2^i, \ldots, \alpha_m^i\}; & i = 1, 2, \ldots, q_0 \\ I; & i = 0 \end{cases} \tag{4.2}$$

$$\begin{cases} 0 < \alpha_k^i < 1, & \text{if the } k^{th} \text{ control surface fails where } k = 1, \ldots, m \\ \alpha_k^i = 1, & \text{if the } k^{th} \text{ control surface does not fail, } k = 1, \ldots, m \end{cases} \tag{4.3}$$

Here the failure times are T_i, $i = 1, \ldots, q_0$; which control surfaces fail at T_i, $i = 1, \ldots, q_0$ is unknown; the amount of the loss of effectiveness at T_i given by α^i, where $\alpha_k^i \in (0, 1)$ is unknown. Furthermore, once a control surface

fails it may fail again later with a different amount of loss of effectiveness.

The plant is augmented with a single fixed feedforward compensator of the form

$$H^{-1}(s) = \frac{K^{-1}}{1+\tau s} \tag{4.4}$$

A state space realization of $H^{-1}(s)$ is given by

$$\dot{s_p}(t) = A_s s_p(t) + B_s u_p(t) \tag{4.5}$$

$$h_p(t) = C_s s_p(t) \tag{4.6}$$

The augmented plant is then given by

$$\mathcal{P}_i^a : \begin{cases} \dot{x}_p^a(t) = A_p^a x_p^a(t) + B_p^a \alpha^i u_p(t) \\ y_p^a(t) = C_p^a x_p^a(t) \end{cases} \tag{4.7}$$

where $x_p^a = \begin{pmatrix} x_p \\ s_p \end{pmatrix}$; $A_p^a = \begin{pmatrix} A_p & 0 \\ 0 & A_s \end{pmatrix}$; $B_p^a \alpha^i = \begin{pmatrix} B_p \alpha^i \\ B_s \end{pmatrix}$;

$C_p^a = (\ C_p \quad C_s\ )$;

and where $x_p^a(t) \in \Re^n$; $u_p(t) \in \Re^m$; and $y_p^a(t) \in \Re^q$.

Then, the augmented output to be controlled is

$$y_p^a(t) = y_p(t) + h_p(t) \tag{4.8}$$

where $h_p(t)$ is the inverse Laplace transform of $H^{-1}(s)$.

Remark 4.1 *We note that the feedforward compensator can be either constant or dynamic.*

The control objective is to design an adaptive control signal $u_p(t)$ such that all signals in the closed loop system are bounded and the augmented plant output $y_p^a(t)$ asymptotically tracks the output of a reference model given by

$$\dot{x}_m(t) = A_m x_m(t) + B_m u_m(t) \tag{4.9}$$

$$y_m(t) = C_m x_m(t) \tag{4.10}$$

where $A_m \in \Re^{n_m \times n_m}$, $B_m \in \Re^{n_m \times m_m}$, $C_m \in \Re^{q \times n_m}$.

Remark 4.2 *We remark that the order of the plant may be much greater than the order of the reference model. Furthermore, we restrict $u_m(t)$ to be a step.*

4.3 Command Generator Tracker Solution for a Known Plant with Unknown Failures

It is useful to incorporate the command generator tracker (CGT) concept developed by O'Brien and Broussard [23]. The CGT is a model reference control law for linear time invariant systems with known coefficients. When

perfect tracking occurs (i.e., $y_p^a = y_m$ for $t \geq 0$), then the corresponding state and control trajectories are defined to be the ideal state and ideal control trajectories, respectively. These ideal trajectories will be denoted by $x_p^*(t)$ and $u_p^*(t)$. The objective is that output of the augmented plant track the output of the reference model. When perfect tracking occurs, $x_p^a = x_p^*$, $u_p = u_p^*$, and

$$\dot{x}_p^* = A_p^a x_p^* + B_p^a \alpha^i u_p^* \tag{4.11}$$

$$y_p^* = C_p^a x_p^* \tag{4.12}$$

It will be assumed that the ideal trajectories are linear functions of the model state and model input. Mathematically:

$$\begin{bmatrix} x_p^* \\ u_p^* \end{bmatrix} = \begin{bmatrix} S_{11} & S_{12} \\ S_{21} & S_{22} \end{bmatrix} \begin{bmatrix} x_m \\ u_m \end{bmatrix} \tag{4.13}$$

Differentiate x_p^* in (4.13)

$\dot{x}_p^* = S_{11}\dot{x}_m + S_{12}\dot{u}_m; \quad \dot{u}_m = 0$

$$\dot{x}_p^* = S_{11}A_m x_m + S_{11}B_m u_m \tag{4.14}$$

$$y_p^* = C_m x_m \tag{4.15}$$

Concatenate (4.11) and (4.12) to obtain

$$\begin{bmatrix} \dot{x}_p^* \\ y_p^* \end{bmatrix} = \begin{bmatrix} A_p^a & B_p^a \alpha^i \\ C_p^a & 0 \end{bmatrix} \begin{bmatrix} x_p^* \\ u_p^* \end{bmatrix} \tag{4.16}$$

$$\begin{bmatrix} \dot{x}_p^* \\ y_p^* \end{bmatrix} = \begin{bmatrix} A_p^a & B_p^a\alpha^i \\ C_p^a & 0 \end{bmatrix} \begin{bmatrix} S_{11} & S_{12} \\ S_{21} & S_{22} \end{bmatrix} \begin{bmatrix} x_m \\ u_m \end{bmatrix} \tag{4.17}$$

Substituting (4.14) and (4.15) in (4.17) yields

$$\begin{bmatrix} S_{11}A_m & S_{11}B_m \\ C_m & 0 \end{bmatrix} \begin{bmatrix} x_m \\ u_m \end{bmatrix} = \begin{bmatrix} A_p^a & B_p^a\alpha^i \\ C_p^a & 0 \end{bmatrix} \begin{bmatrix} S_{11} & S_{12} \\ S_{21} & S_{22} \end{bmatrix} \begin{bmatrix} x_m \\ u_m \end{bmatrix} \tag{4.18}$$

Since x_m and u_m are arbitrary, (4.18) is satisfied if:

$$\begin{bmatrix} S_{11}A_m & S_{11}B_m \\ C_m & 0 \end{bmatrix} = \begin{bmatrix} A_p^a & B_p^a\alpha^i \\ C_p^a & 0 \end{bmatrix} \begin{bmatrix} S_{11} & S_{12} \\ S_{21} & S_{22} \end{bmatrix} \tag{4.19}$$

Rewrite (4.19) to obtain

$$\begin{cases} (A_p^a S_{11} + B_p^a\alpha^i S_{21}) = S_{11}A_m \\ (A_p^a S_{12} + B_p^a\alpha^i S_{22}) = S_{11}B_m \\ C_p^a S_{11} = C_m \\ C_p^a S_{12} = 0 \end{cases} \tag{4.20}$$

where $S_{11} \in \Re^{n\times n_m}$; $S_{12} \in \Re^{n\times m_m}$; $S_{21} \in \Re^{m\times n_m}$; $S_{22} \in \Re^{m\times m_m}$.

Therefore, we have $nn_m + nm_m + mn_m + 2mm_m$ unknowns and $nn_m + nm_m + qn_m + 2qm_m$ equations.

Remark 4.3 *When m, the number of controls, is greater than or equal to q, the number of outputs to be controlled, there are at least as many unknowns as equations. For this reason, the CGT solution almost always exists.*

A more elegant, but not always solvable approach, is to define

$$\begin{bmatrix} \Omega_{11} & \Omega_{12} \\ \Omega_{21} & \Omega_{22} \end{bmatrix} = \begin{bmatrix} A_p^a & B_p^a \alpha^i \\ C_p^a & 0 \end{bmatrix}^{-1} \tag{4.21}$$

Then the partitioned matrix equations to be solved are

$$\begin{cases} S_{11} = \Omega_{11} S_{11} A_m + \Omega_{12} C_m \\ S_{12} = \Omega_{11} S_{11} B_m \\ S_{21} = \Omega_{21} S_{11} A_m + \Omega_{22} C_m \\ S_{22} = \Omega_{21} S_{11} B_m \end{cases} \tag{4.22}$$

Remark 4.4 *The existence of the inverse in (4.21) requires that $q = m$. If $m > q$, a pseudoinverse may be required, where as the case $m < q$ does not usually have a solution.*

Note that the first equation in (4.22) is a Lyapunov equation, the solution of which exists if Ω_{11} has no eigenvalue which is the inverse of any eigenvalue of A_m. It can be shown that the inverse of the eigenvalues of Ω_{11} are the transmission zeros of the augmented plant. Therefore, if the, augmented plant does not have a transmission zero at the origin and if no transmission zero of the augmented plant is equal to an eigenvalue of the reference model, then the first equation in (4.22) has a solution [23].

4.4 Adaptive Control Algorithm

The adaptive control law that forces the augmented plant output given by (4.7) to track the reference model output given by (4.10) is

$$u_p(t) = K_x x_m(t) + K_u u_m(t) + K_e[y_m(t) - y_p^a(t)] \tag{4.23}$$

where K_x, K_u, and K_e are adaptive gains.

The adaptive gains are concatenated into matrix $K_r(t)$ defined as

$$K_r(t) = [K_e(t), K_x(t), K_u(t)] \tag{4.24}$$

The concatenated gain $K_r(t)$ is defined as the sum of a proportional gain $K_p(t)$ and an integral gain $K_I(t)$, each of which is adapted as follows:

$$K_r(t) = K_p(t) + K_I(t) \tag{4.25}$$

$$K_p(t) = e_y^a(t) r^T(t) \bar{T} \tag{4.26}$$

$$\dot{K}_I(t) = e_y^a(t) r^T(t) T \tag{4.27}$$

$$r^T(t) = [(e_y^a)^T(t), x_m^T(t), u_m^T(t)] \tag{4.28}$$

$$e_y^a(t) = y_m(t) - y_p^a(t) \tag{4.29}$$

where T, $\bar{T}$ are time invariant weighting matrices, and $e_y^a(t)$ denotes the augmented output error.

The error equation is derived in Appendix D and is given by

$$\dot{e}_x = A_c e_x - B_p^a \alpha^i [K_r - \tilde{K}_i] r \tag{4.30}$$

where $A_c = A_p^a - B_p^a \alpha^i \tilde{K}_{ei} C_p^a$ and where $\tilde{K}_i = [\tilde{K}_{ei}, \tilde{K}_{xi}, \tilde{K}_{ui}]$ are constant gains which are not needed for implementation.

4.5 Stability Analysis

In this section, we present two lemmas and one theorem describing the stability of the adaptive controller. Lemma 4.1 shows that positive definite quadratic Lyapunov functions exist such that their derivatives are negative semi definite. Lemma 4.2 describes a sufficient condition for the boundedness of the Lyapunov functions at the failure instants. This condition limits the loss of control effectiveness failure to 50%. However, it will be shown via simulation that this is only a sufficient condition and that we still can accommodate more that 50% of loss of control effectiveness. Theorem 4.1 shows the boundedness of all states and gains in the adaptive loop and that the augmented output error vanishes asymptotically.

Lemma 4.1 *If the augmented plant $\mathcal{P}_i^a$ is ASPR , i.e., there exist positive*

definite matrices P_i, Q_i, and a gain matrix $\tilde{K}_{ei}$ such that:

$$P_i(A_p^a - B_p^a\alpha^i\tilde{K}_{ei}C_p^a) + (A_p^a - B_p^a\alpha^i\tilde{K}_{ei}C_p^a)^T P_i = -Q_i < 0 \qquad (4.31)$$

$$(C_p^a)^T = P_i B_p^a \alpha^i \qquad (4.32)$$

and if $dim[y_p^a(t)] \leq dim[u_p(t)]$ and T and $\bar{T}$ positive definite symmetric, then a positive definite quadratic Lyapunov function $V_i(e_x, K_I)$ can be selected such that its derivative $\dot{V}_i$ is negative semi-definite for $t \in (T_i, T_{i+1})$, $i = 0, 1, 2, \ldots, q_0$.

Proof: See Appendix E.

Remark 4.5 *We present an overview of the proof of Lemma 4.1. Choose the positive definite quadratic Lyapunov function as*

$$V_i(e_x, K_I) = e_x^T P_i e_x + tr[(K_I - \tilde{K}_i)T^{-1}(K_I - \tilde{K}_i)^T] \qquad (4.33)$$

then, the derivative of (4.33) along the trajectories of Eq. (4.30) is

$$\dot{V}_i = -e_x^T Q_i e_x - 2(e_y^a)^T e_y^a r^T \bar{T} r \leq 0; \; t \in (T_i, T_{i+1}) \qquad (4.34)$$

Hence, $\dot{V}_i$ is negative semidefinite in (e_x, K_I) for $t \in (T_i, T_{i+1})$.

Lemma 4.2 *Let $V_i(t) \equiv V_i(e_x(t), K_I(t))$. If $\alpha_k^i \geq \frac{1}{2}$, $k = 1, 2, \ldots, m$, $i = 1, 2, \ldots, q_0$; then, the Lyapunov functions at the failure instants given by $V_i(T_i)$, $i = 1, 2, \ldots, q_0$ are bounded.*

Proof: See Appendix F

Remark 4.6 *We present an overview of the proof of Lemma 4.2. Consider the first failure at* $t = T_1$. *We show in appendix F that* $V_1(T_1) \leq 2V_0(T_1) + e_x^T(P_1 - 2P_0)e_x + 2\Delta V_1$ *where* ΔV_1 *is constant.* $V_0(T_1)$ *is bounded because* $V_0(t)$ *is monotone nonincreasing for* $t \in [0, T_1)$ *and* $V_0(0)$ *is bounded. We show that* $\alpha_k^i \geq \frac{1}{2}, \quad k = 1, \ldots, m$ *implies that* $e_x^T(P_1 - 2P_0)e_x \leq 0$. *Hence* $V_1(T_1)$ *is bounded. This argument can be extended to obtain* $V_i(T_i) \leq \eta V_0(0) + \beta$ *where* η *and* β *are constants.*

Theorem 4.1 *If*

1. *the augmented plant* $\mathcal{P}_i^a$ *is ASPR,* $i = 0, 1, 2, \ldots, q_0$
2. $dim[y_p^a(t)] \leq dim[u_p(t)]$
3. T *and* $\bar{T}$ *are positive definite symmetric*
4. *all* $\alpha_k^i \geq \frac{1}{2}, \quad k = 1, 2, \ldots, m; \quad i = 1, 2, \ldots, q_0$

   then all states and gains in the adaptive loop are bounded, and the augmented output error vanishes asymptotically.

Proof: The boundedness of all states and gains follows from Lemmas 4.1 and 4.2. The proof that the augmented output error vanishes is shown in Appendix G.

4.6 Feedforward Design

We propose a method which uses the MATLAB® LMI Toolbox [14] and the MATLAB® Optimization Toolbox [15] to design a robust feedforward compensator. Each augmented LTI plant $\mathcal{P}_i^a$, $i = 0, 1, \ldots, q_0$ must be ASPR using the same feedforward. However, we do not know in advance which failures will occur.

Suppose there are j_0 possible failure configurations $\mathcal{P}_j$, $j = 1, \ldots, j_0$. Each possible failure configuration $\mathcal{P}_j$ corresponds to one surface failure, or two simultaneous surface failures, or three simultaneous surface failures, and so on. The $\mathcal{P}_j$'s are parameterized by a range of possible control effectiveness loss. Thus, the $\mathcal{P}_j$'s are different from the $\mathcal{P}_i$'s in Eq. (4.1) because the $\mathcal{P}_i$'s uniquely define a failure whereas the $\mathcal{P}_j$'s define a possible parameterized failure configuration. Also, let (A_p, B_p^0, C_p) correspond to the unfailed plant.

Consider an affine parameter dependent representation of $\mathcal{P}_j$ given by

$$\mathcal{P}_j(\sigma): \begin{cases} \dot{x}_p &= A_p x_p + B_p^j(\sigma) u_p \\ y_p &= C_p x_p \end{cases} \tag{4.35}$$

where $B_p^j(\sigma) = B_p^0 - \sum_{k=1}^{k_j} \sigma_k^j B_k^j$, $j = 1, \ldots, j_0$ and where k_j is the number of surfaces of $\mathcal{P}_j(\sigma)$ which simultaneously fail. Here B_k^j describes the failure

of one surface and σ_k^j describes the corresponding range of control effectiveness loss. Typically $\sigma_k^j \in [0, \frac{1}{2}]$ because of the result in Lemma 4.2.

The following two lemmas due to Barkana [24] show that the feedforward compensator for a strictly proper plant has a simple form.

Lemma 4.3 *[24] Let $G(s)$ be any $m \times m$ strictly proper transfer matrix of arbitrary McMillan degree. $G(s)$ is not necessarily stable or minimum phase. Let K be a nonsingular constant output feedback matrix such that the closed loop transfer matrix*

$$G_{cl}(s) = [I + G(s)K]^{-1}G(s) \tag{4.36}$$

is asymptotically stable. Then, the augmented open loop transfer matrix

$$G_a(s) = G(s) + K^{-1} \tag{4.37}$$

is ASPR.

Lemma 4.4 *[24] Let $G(s)$ be any $m \times m$ strictly proper transfer matrix of arbitrary McMillan degree. $G(s)$ is not necessarily stable or minimum phase. Let $H(s) = K(1 + \tau s)$ be a stabilizing closed loop compensator of $G(s)$. Then, the augmented plant*

$$G_a(s) = G(s) + H^{-1}(s) = G(s) + \frac{K^{-1}}{1 + \tau s} \tag{4.38}$$

is ASPR.

We want to minimize the norm of K^{-1} so that

$$y_p^a(t) = y_p(t) + h_p(t) \approx y_p(t) \tag{4.39}$$

while ensuring that K robustly stabilizes every $\mathcal{P}_j(\sigma)$ $j = 1, \ldots, j_0$

Let $\tilde{\mathcal{P}}_j(\sigma)$ be $\mathcal{P}_j(\sigma)$ with feedback K $j = 1, \ldots, j_0$

Mathematically

$$\min_K \| K^{-1} \|_F \ s.t \ \tilde{\mathcal{P}}_j(\sigma) \ is \ robustly \ stable; \ j = 1, \ldots, j_0 \tag{4.40}$$

We ensure that the $\tilde{\mathcal{P}}_j(\sigma)$'s are robustly stable by using program *"pdlstab"* from the MATLAB® LMI Toolbox [14] and program *"fmincon"* from the MATLAB® Optimization Toolbox [15]. At each iteration of the optimization, we call *"pdlstab"* once for each $\tilde{\mathcal{P}}_j(\sigma)$, $j = 1, \ldots, j_0$. We require that the quantities t_{min}^j; $j = 1, \ldots, j_0$ be negative. Here t_{min}^j is computed by *"pdlstab"* where $t_{min}^j < 0$ ensures the existence of a parameter dependent Lyapunov function for $\tilde{\mathcal{P}}_j(\sigma)$. With $t_{min}^j < 0$, $j = 1, \ldots, j_0$ every LTI plant which belongs to $\tilde{\mathcal{P}}_j(\sigma)$, $j = 1, \ldots, j_0$ is stable. We remark that on each interval $t \in (T_i, T_{i+1})$ we have an LTI plant $\mathcal{P}_i$, $i = 1, \ldots, q_0$. Let $\tilde{\mathcal{P}}_i$ be the LTI plant $\mathcal{P}_i$ with feedback K. Then, every LTI plant $\tilde{\mathcal{P}}_i$ is one of the $\tilde{\mathcal{P}}_j(\sigma)$ for some values of j and σ. Thus, every LTI plant $\tilde{\mathcal{P}}_i$ is stable. Then, it follows that

every augmented plant $\mathcal{P}_i^a$, $i = 1,\ldots,q_0$ is ASPR.

Remark 4.7 *The system in (4.35) with feedback* $H(s) = K(1+\tau s)$ *is given by*

$$\dot{x}_p = A_{cl}^j(\sigma)x_p \tag{4.41}$$

where

$$A_{cl}^j(\sigma) = A_p - B_p^j(\sigma)[I+\tau KC_pB_p^j(\sigma)]^{-1}KC_p(I+\tau A_p) \tag{4.42}$$

which we observe is not affine in $B_p^j(\sigma)$ *as required by program "pdlstab". However, the closed loop system matrix with constant feedback K is given by*

$$A_{cl}^j(\sigma) = A_p - B_p^j(\sigma)KC_p \tag{4.43}$$

which is affine in $B_p^j(\sigma)$.

This is the reason that we use "pdlstab" to compute a stabilizing constant feedback K instead of the dynamic feedback $K(1+\tau s)$.

Remark 4.8 *The implementation of a constant feedforward* K^{-1} *yields an algebraic loop which causes a problem in the computer simulation. Therefore, we first compute a constant gain K which stabilizes* $A_{cl}^j(\sigma)$ *in (4.43) for all j and* σ *by using* "pdlstab" *and* "fmincon". *Then, we implement the*

feedforward $H^{-1}(s) = \frac{K^{-1}}{1+\tau s}$ *where* τ *is sufficiently small. We show in Theorem 4.2 that such a* τ *exists so that* $H(s) = K(1+\tau s)$ *stabilizes* $A_{cl}^{j}(\sigma)$ *in (4.42) for all* j *and* σ. *Therefore,* $H^{-1}(s) = \frac{K^{-1}}{1+\tau s}$ *satisfies lemma 4.4.*

The following theorem is proposed in collaboration with Piou (2003) [25].

Theorem 4.2 *Suppose* $A_{cl}^{j}(\sigma)$ *in (4.43) is stable with a non-defective modal matrix for all* j *and* σ. *Then, there exists* τ *sufficiently small such that* $A_{cl}^{j}(\sigma)$ *in (4.42) is stable for all* j *and* σ.

Proof: See Appendix H.

4.7 Example

We consider the linearized lateral dynamics of the F/A-18A aircraft. The rigid body states are lateral velocity(v), yaw rate (r), roll rate (p), and bank angle (ϕ). The control surface deflections are asymmetric trailing edge flaps (δ_{te}), ailerons (δ_a), and rudder (δ_r). The measurements are sideslip angle (β), washed out yaw rate (r_{wo}), and roll rate(p). The unfailed aircraft is described by the triple (A_p, B_p^0, C_p). The state matrices A_p, B_p^0, C_p are shown below

$$A_p = \begin{bmatrix} -0.245 & -646.9 & 0.0285 & 32.189 & 0 \\ 0.00849 & -0.2460 & 0.112 & 0 & 0 \\ -0.0256 & 0.73 & -2.83 & 0 & 0 \\ 0 & 0 & 1 & 0 & 0 \\ 0 & 0.5 & 0 & 0 & -0.5 \end{bmatrix} \quad (4.44)$$

$$B_p^0 = \begin{bmatrix} 0 & -2.915 & 34.909 \\ -0.835 & -0.896 & -3.26 \\ 13.06 & 13.14 & 4.4 \\ 0 & 0 & 0 \\ 0 & 0 & 0 \end{bmatrix} \quad (4.45)$$

$$C_p = \begin{bmatrix} 1/650 & 0 & 0 & 0 & 0 \\ 0 & 1 & 0 & 0 & -1 \\ 0 & 0 & 1 & 0 & 0 \end{bmatrix} \quad (4.46)$$

The block diagram of the adaptive control system is shown in Figure 4.1.

An output feedback gain matrix K_{eig} is designed using eigenstructure assignment for the unfailed aircraft by assigning the dutch roll mode to have a damping of 0.707 and a natural frequency of 2.83 r/s. The roll subsidence

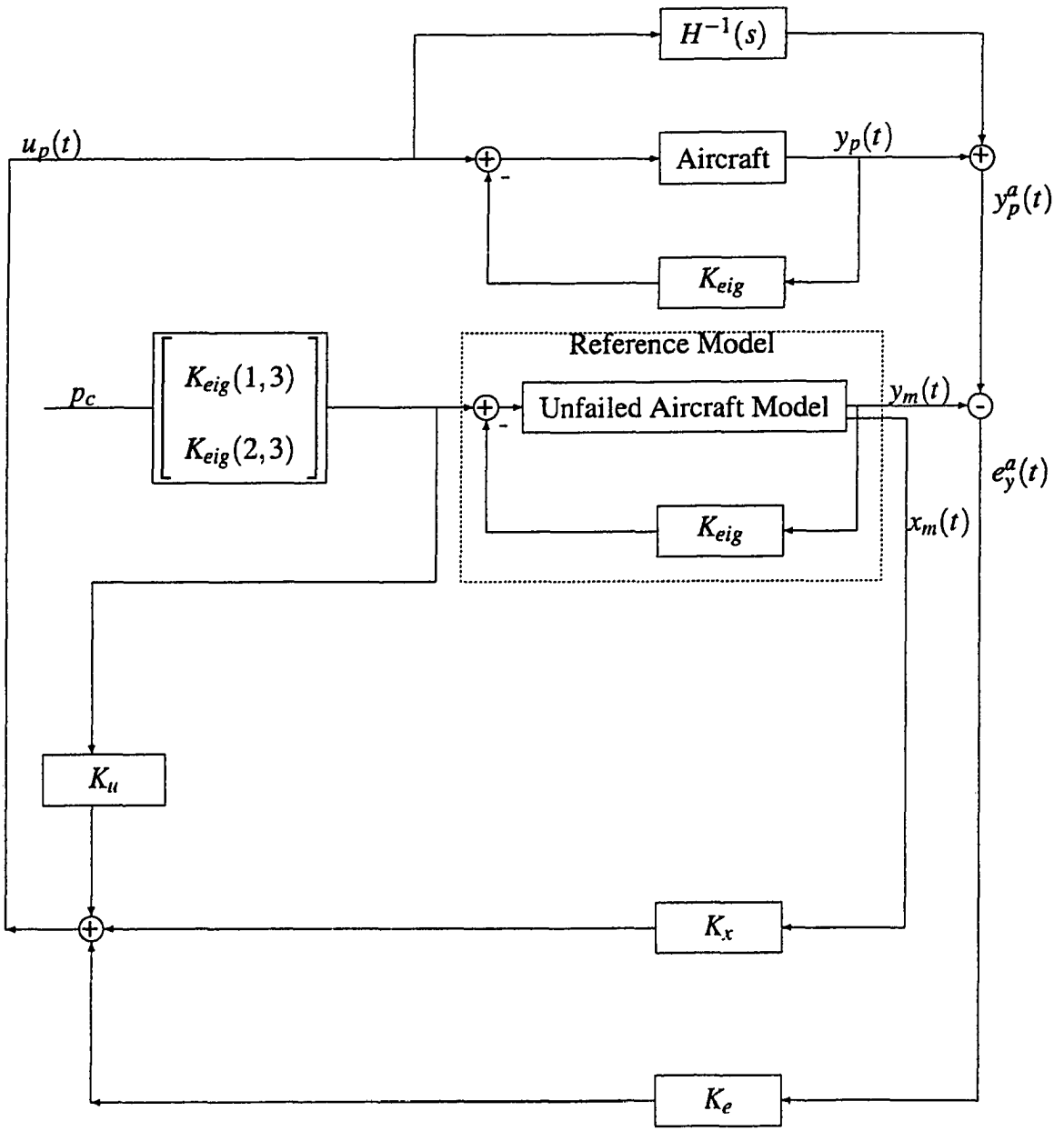

Figure 4.1: Block Diagram of Adaptive Control System

mode is assigned to -4. The desired eigenstructure and the feedback gain matrix K_{eig} are shown in Table 4.1. The reference model open loop and closed loop eigenvalues are shown in Table 4.2. From Table 4.2, we observe that the closed loop spiral mode is unstable. However, this instability is within the limits of MIL-F-8785C specifications which specifies that the spiral minimum time to double amplitude is 12 seconds.

Table 4.1: Desired Eigenstructure and Feedback Gain Matrix K_{eig}

Dutch Roll	Roll subsidence		K_{eig}			
$\lambda_{dr} = -2 \pm 2j$	$\lambda_{roll} = -4$		β	r_{wo}	p	
$1 + j$x	0	v	-1.8768	0.4583	0.1111	δ_{ac}
x$+ j1$	0	r	1.7234	-1.2	-0.0656	δ_{rc}
$0 + j0$	1	p				
$0 + j0$	x	ϕ				
x$+ j$x	0	x_5				

The achievable eigenvectors, which were computed using the default value for *TOL* in MATLAB® function *"pinv"*, are shown in Table 4.3. We observe that the assigned entries of the dutch roll and roll subsidence eigenvectors have been achieved almost exactly.

Here we only use rudder and aileron because these two control surfaces are sufficient to achieve desired handling qualities for the unfailed aircraft.

Table 4.2: Reference Model Open loop and Closed Loop Eigenvalues

Open Loop Eigenvalues	Closed Loop Eigenvalues	Modes
-0.5	-0.6035	Filter
$-0.2804+2.2877j$	$-2.0000+2.0000j$	Dutch Roll
$-0.2804-2.2877j$	$-2.0000-2.0000j$	Dutch Roll
-2.7599	-4.0000	Roll Subsidence
-0.0002	0.0090	Spiral

However, the adaptive controller will use all three control surfaces in order to accommodate failures. The open and closed loop time responses of the reference model to a one degree initial sideslip are shown in Figures 4.2, and 4.3, respectively. Observe that the reference model exhibits desirable damping and sideslip to bank decoupling.

Table 4.3: Achievable Eigenvectors

Dutch Roll	Roll subsidence	
$\lambda_{dr}=-2\pm 2j$	$\lambda_{roll}=-4$	
$1+j358.0777$	0.0001	v
$1.1878+j1$	-0.009	r
$0+j0$	0.9999	p
$0+j0$	-0.25	ϕ
$0.0175-j0.3101$	0.0013	x_5

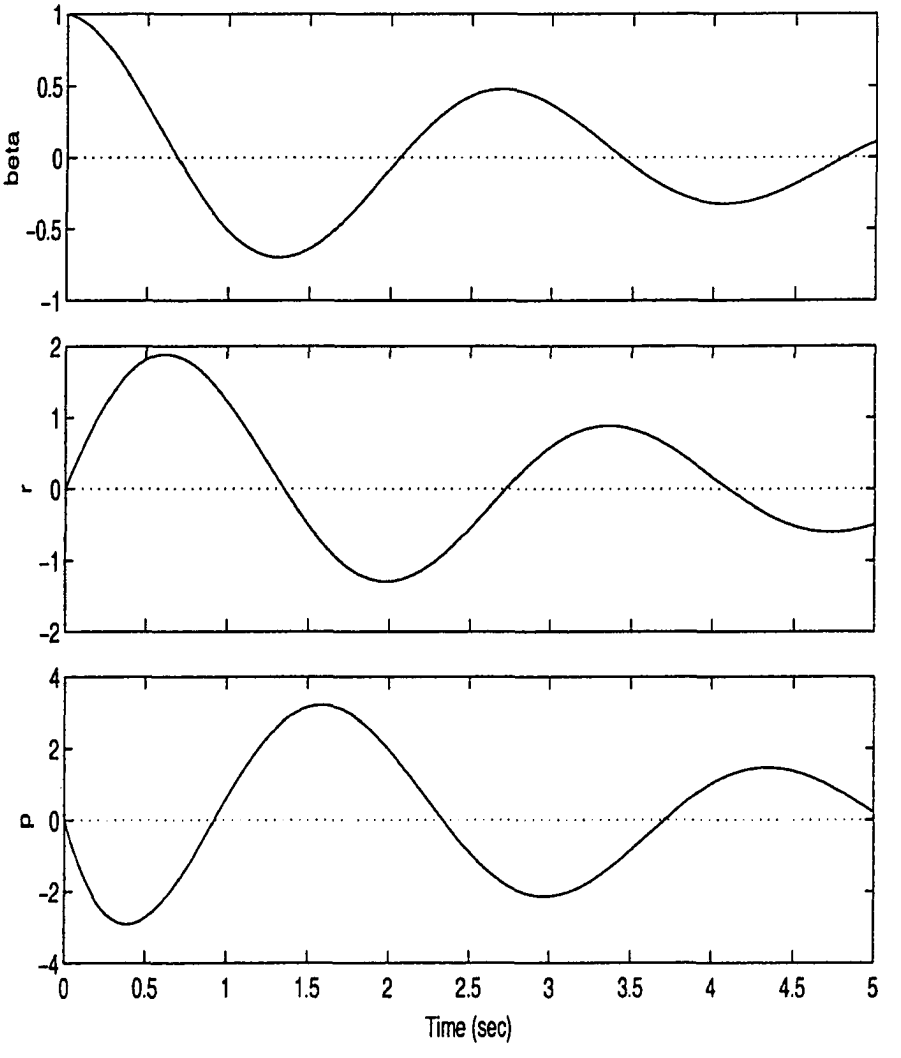

Figure 4.2: Open Loop Time Responses to One Degree Initial Sideslip Angle

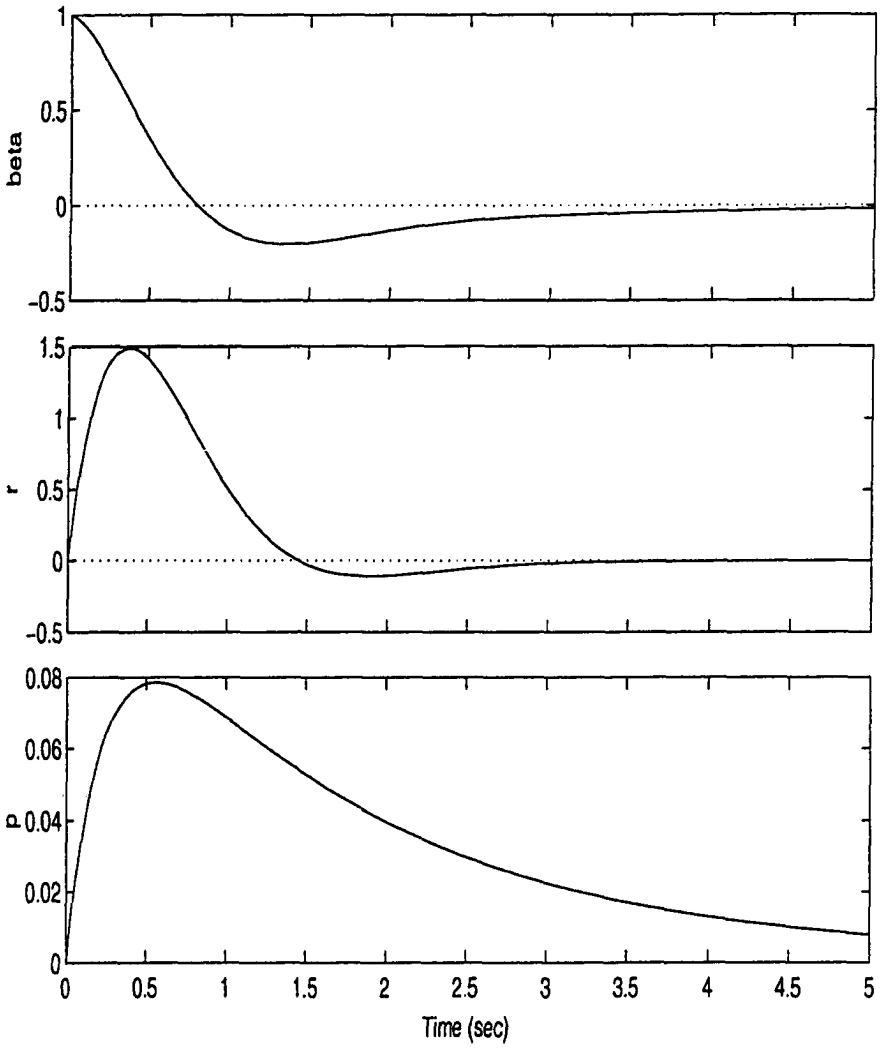

Figure 4.3: Closed Loop Time Responses to One Degree Initial Sideslip Angle

The unfailed aircraft with feedback K_{eig} is not ASPR because there are two transmission zeros at $z_1 = 0.2028 \times 10^{-13}$; and $z_2 = -0.0002 \times 10^{-13}$ one of which is non-minimum phase. The feedforward which satisfies the ASPR condition will be designed for the unfailed aircraft with feedback K_{eig}. This closed loop unfailed aircraft is described by the triple $(A_p - B_p^0 K_{eig} C_p, B_p^0, C_p)$. The reference model is chosen to be the same triple so that $A_m = A_p - B_p^0 K_{eig} C_p$, $B_m = B_p^0$, and $C_m = C_p$. Thus, when there are no failures the reference model is the aircraft with eigenstructure assignment feedback K_{eig}. Next, we show how the reference model input u_m is computed.

$$u_m = -K_{eig}(y_m - y_c) \tag{4.47}$$

$$= -K_{eig} \begin{bmatrix} \beta \\ r_{wo} \\ p - p_c \end{bmatrix} \tag{4.48}$$

$$= -\begin{bmatrix} K_{eig}(1,1) & K_{eig}(1,2) & K_{eig}(1,3) \\ K_{eig}(2,1) & K_{eig}(2,2) & K_{eig}(2,3) \end{bmatrix} \begin{bmatrix} \beta \\ r_{wo} \\ p - p_c \end{bmatrix} \tag{4.49}$$

$$= -K_{eig} y_m + \begin{bmatrix} K_{eig}(1,3) \\ K_{eig}(2,3) \end{bmatrix} p_c \tag{4.50}$$

We use Eq. (4.50) to implement the reference model in Figure 4.1 where p_c

is the pilot roll rate command.

We design a robust feedforward so that the aircraft with feedback K_{eig} and feedforward K^{-1} is ASPR for all possible failures. The affine parameter dependent representation of the aircraft with feedback gain K_{eig} is described by the triple $(A_p - B_p^j(\sigma)K_{eig}C_p, B_p^j(\sigma), C_p)$. It can be shown that the closed loop system for $(A_p - B_p^j(\sigma)K_{eig}C_p, B_p^j(\sigma), C_p)$ with feedback gain K is given by

$$\dot{x}_p = A_{cl}^j(\sigma)x_p \tag{4.51}$$

where

$$A_{cl}^j(\sigma) = A_p - B_p^j(\sigma)[K_{eig} + K]C_p \tag{4.52}$$

The feedback gain K is computed so that Eq. (4.51) is stable for all possible failures.

We perform the optimization in Eq. (4.40) by using program *"fmincon"* from the MATLAB® Optimization Toolbox [15] and program *"pdlstab"* from the MATLAB® LMI Toolbox [14]. We use *"fmincon"* to minimize the Frobenius norm of K^{-1} as shown in Eq. (4.40).

We choose the possible failures to be the loss of control effectiveness of any one surface. However, we do not know which control surface will fail nor do we know the amount of control effectiveness loss. We have three failure cases where each failure case corresponds to one control surface failure. Thus, $B_p^j(\sigma)$ in Eq. (4.35) becomes

$$B_p^j(\sigma) = B_p^0 - \sigma_1^j B_1^j \quad j = 1,\ldots,3 \tag{4.53}$$

where

$$B_1^1 = B_p^0 diag\{1\ 0\ 0\};\ j = 1 \tag{4.54}$$

$$B_1^2 = B_p^0 diag\{0\ 1\ 0\};\ j = 2 \tag{4.55}$$

$$B_1^3 = B_p^0 diag\{0\ 0\ 1\};\ j = 3 \tag{4.56}$$

Then

$$A_{cl}^j(\sigma) = A_p - (B_p^0 - \sigma_1^j B_1^j)(K_{eig} + K)C_p \tag{4.57}$$

$$= [A_p - B_p^0(K_{eig} + K)C_p] + \sigma_1^j B_1^j (K_{eig} + K)C_p \tag{4.58}$$

Finally, the closed loop matrices for the three failure cases are given by:

Trailing Edge Flap Failure ($j = 1$)

$$A_{cl}^1(\sigma) = [A_p - B_p^0(K_{eig} + K)C_p] + \sigma_1^1 B_1^1 (K_{eig} + K)C_p \tag{4.59}$$

$$= A_0^1 + p_1^1 A_1^1 \tag{4.60}$$

where

$$A_0^1 = [A_p - B_p^0(K_{eig} + K)C_p] \tag{4.61}$$

$$A_1^1 = B_1^1(K_{eig} + K)C_p \tag{4.62}$$

$$p_1^1 = \sigma_1^1 \tag{4.63}$$

Aileron Failure ($j = 2$)

$$A_{cl}^2(\sigma) = [A_p - B_p^0(K_{eig} + K)C_p] + \sigma_1^2 B_1^2(K_{eig} + K)C_p \tag{4.64}$$

$$= A_0^2 + p_1^2 A_1^2 \tag{4.65}$$

where

$$A_0^2 = [A_p - B_p^0(K_{eig} + K)C_p] \tag{4.66}$$

$$A_1^2 = B_1^2(K_{eig} + K)C_p \tag{4.67}$$

$$p_1^2 = \sigma_1^2 \tag{4.68}$$

Rudder Failure ($j = 3$)

$$A_{cl}^3(\sigma) = [A_p - B_p^0(K_{eig} + K)C_p] + \sigma_1^3 B_1^3(K_{eig} + K)C_p \tag{4.69}$$

$$= A_0^3 + p_1^3 A_1^3 \tag{4.70}$$

where

$$A_0^3 = [A_p - B_p^0(K_{eig} + K)C_p] \tag{4.71}$$

$$A_1^3 = B_1^3(K_{eig} + K)C_p \tag{4.72}$$

$$p_1^3 = \sigma_1^3 \tag{4.73}$$

Our experience indicates that the optimization should be initialized with a nonsingular stabilizing gain. We compute this initial gain, denoted by $K_{initial}$, by using eigenstructure assignment. This gain uses all three control surfaces because the adaptive controller will use all three control surfaces. The desired eigenvalues and eigenvectors are the same that were used to compute K_{eig}. We attempted to obtain $K_{initial}$ using eigenstructure assignment, but the unassigned eigenvalues were unstable. The (5×3) control distribution matrix B_p^0 has singular values 35.3966, 18.6783, and 0.2101. The small singular value, which corresponds to a direction of weak control, causes some of the feedback gains to be on the order of 10^4. The physical explanation is that even with three control surfaces we can still only generate yawing moment and rolling moment. To alleviate this design problem, we use the pseudo-control strategy of Sobel and Lallman [18]. We choose the columns of the new control distribution matrix $\tilde{B}_p^0$ to be the two singular vectors corresponding to the two larger singular values and use eigenstructure assignment to compute a (2×3) feedback gain matrix. Then, this (2×3) feedback gain is mapped back to the original matrix B_p^0 to obtain the (3×3) gain $K_{initial}$. The designer must be careful when computing the achievable dutch roll eigenvectors because the pseudo-inverse of an ill-conditioned matrix is required. This ill-conditioned matrix has singular

values given by 1.0000, 1.0000, 0.9998, and 0.0028. The achievable eigenvectors were computed using MATLAB® function *"pinv"* with TOL=0.01. This has the effect of discarding the singular value at 0.0028 in the pseudo-inverse computation. The initial feedforward gain $K_{initial}$ is shown in Table 4.4.

Table 4.4: Initial and Optimal Gain Matrices

$K_{initial}$			$K_{optimal}$			
β	r_{wo}	p	β	r_{wo}	p	
1.6456	-0.6527	-0.0067	75.224	15.937	17.504	δ_{te}
1.7811	-0.6997	-0.0072	22.535	-34.857	19.305	δ_a
-0.9257	0.2858	0.003	67.391	-43.849	-14.24	δ_r

We design a feedforward which allows up to 80% loss of control effectiveness in any one control surface. We remark that Lemma 4.2 requires $\alpha_k^j \geq \frac{1}{2}$. However, we will show via simulation that we can accommodate failures of more than 50%. This is because Lemma 4.2 is only a sufficient condition and it is probably conservative. Therefore, the loss of control effectiveness parameters p_1^j are chosen to be $p_1^j \in [0, 0.8]$; $j = 1, \ldots, 3$. We optimize over K as shown in (4.40). The optimization converges with $||K^{-1}||_F = 0.83746$.

We restart the optimization with the final gain as the new initial gain. Then, the optimization converges to a new gain with $\|K^{-1}\|_F = 0.19365$. We repeat this restart process until $\|K^{-1}\|_F$ has only a small change on successive optimizations. This required a total of five optimization runs which includes four restarts. The optimal robust stabilizing gain $K_{optimal}$ is shown in Table 4.4. The Frobenius norm has been reduced from $\| K^{-1}_{initial} \|_F = 1.2 \times 10^5$ to $\| K^{-1}_{optimal} \|_F = 0.042809$ and robust stability is ensured because all t^j_{min} are negative. Hence, lemma 4.3 ensures that the aircraft with feedback K_{eig} and feedforward $K^{-1}_{optimal}$ is ASPR for all control surface failures which belong to the set represented by $p^j_1 \in [0, 0.8]$; $j = 1, \ldots, 3$. However, we add dynamics so that the plant is augmented with a dynamic feedforward compensator $H^{-1}(s) = \frac{K^{-1}_{optimal}}{1+\tau s}$ where $\tau = 10^{-16}$ rather than with constant feedforward $K^{-1}_{optimal}$. This eliminates the algebraic loop associated with the use of a constant feedforward compensator. Finally, we remark that we used version 2.2 of the Optimization Toolbox and version 1.0.8 of the LMI Toolbox. Earlier versions of the toolboxes may produce different answers for $K_{optimal}$.

The pilot command p_c is chosen to be a roll rate step of 10 deg/sec. The initial conditions on both the aircraft and reference model are zero. A control surface failure occurs at t=1 second. We perform a non-adaptive simulation

of the aircraft with the fixed eigenstructure assignment feedback gain K_{eig} for a 50% aileron failure. This corresponds to $K_x = K_e = 0$, $K_u = I$, and $H^{-1}(s)$ is omitted. The aircraft and reference model responses are shown in Figure 4.4. Observe the poor model following in sideslip angle, yaw rate, and roll rate. Here we plot the true yaw rate (r), but recall that we feed back the washed out yaw rate (r_{wo}).

Next, we perform simulations of the adaptive system of Figure 4.1. We initialize the adaptive gains to be $K_x = K_e = 0$ *and* $K_u = I$. This choice of initial gains corresponds to the eigenstructure assignment feedback which was designed for the unfailed aircraft. The weighting matrices T and $\bar{T}$ are chosen to be $T = \bar{T} = I$. The aircraft and reference model responses are shown in Figure 4.5. Observe the almost perfect tracking for sideslip angle, yaw rate, and roll rate as compared to the fixed gain controller.

The time responses for an 80% aileron failure using the fixed eigenstructure assignment feedback gain K_{eig} are shown in Figure 4.6. Observe the poor model following in sideslip angle, yaw rate, and roll rate. Next, we perform simulations of the adaptive system of Figure 4.1 where T and $\bar{T}$ are again chosen to be $T = \bar{T} = I$. The time responses are in Figure 4.7.

Observe the almost perfect tracking for sideslip, yaw rate, and roll rate.

The time responses for a 50% rudder failure using the fixed eigenstructure assignment feedback gain K_{eig} are shown in Figure 4.8. Next, we perform simulations of the adaptive system of Figure 4.1 where T and $\bar{T}$ are again chosen to be $T = \bar{T} = I$. The time responses are shown in Figure 4.9. We observe that the adaptive controller yields almost perfect tracking whereas the fixed gain controller does not. Finally, the time responses for an 80% rudder failure for the fixed gain and adaptive controller are shown in Figures 4.10 and 4.11, respectively.

We observe that the adaptive controller provides almost perfect tracking even though the amount of control effectiveness loss exceeds the value of 50% which is allowed in Lemma 4.2. Finally, we remark that the same chosen T and $\bar{T}$ must be used for all simulations because we do not know in advance which failure will occur.

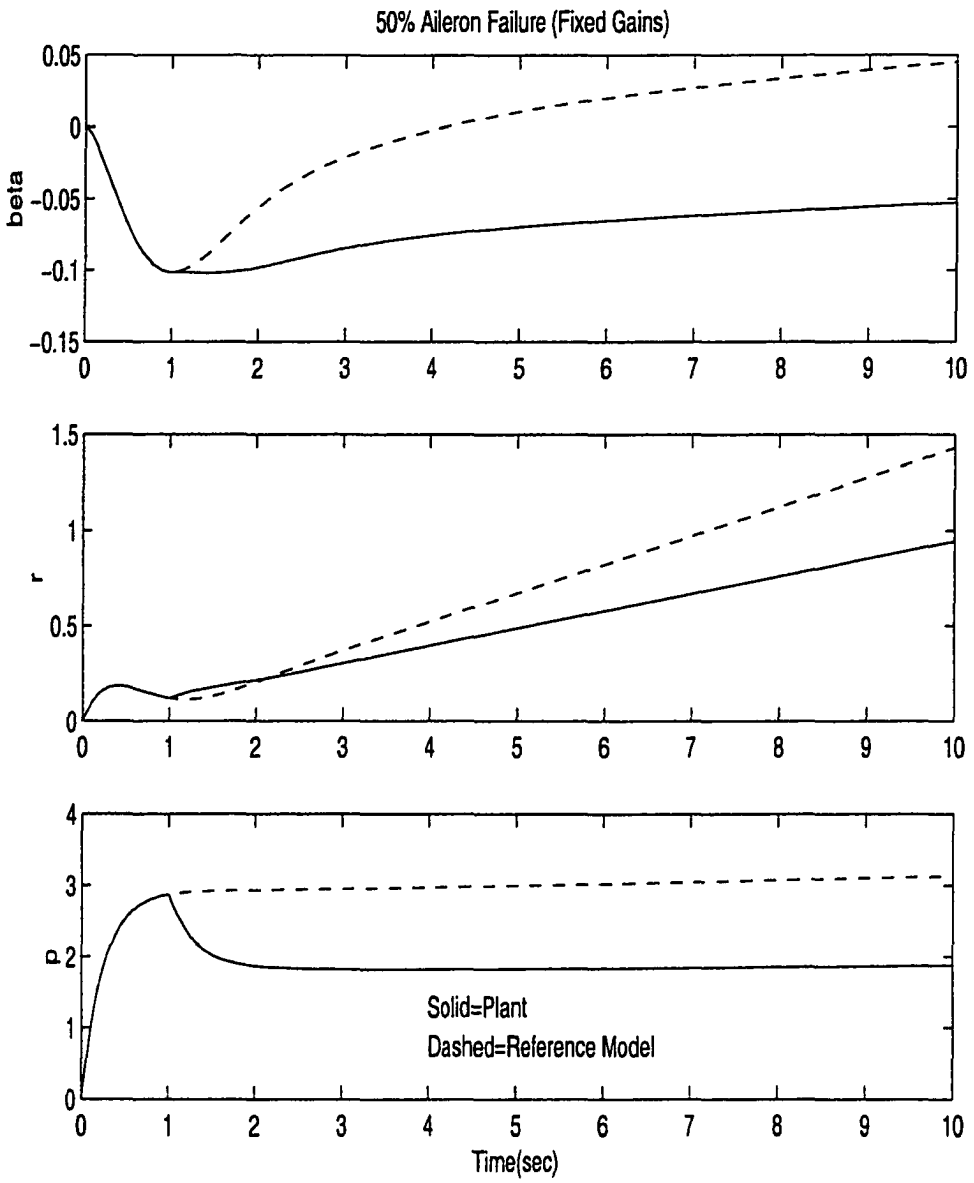

Figure 4.4: 50% Aileron Failure Using Fixed Gains

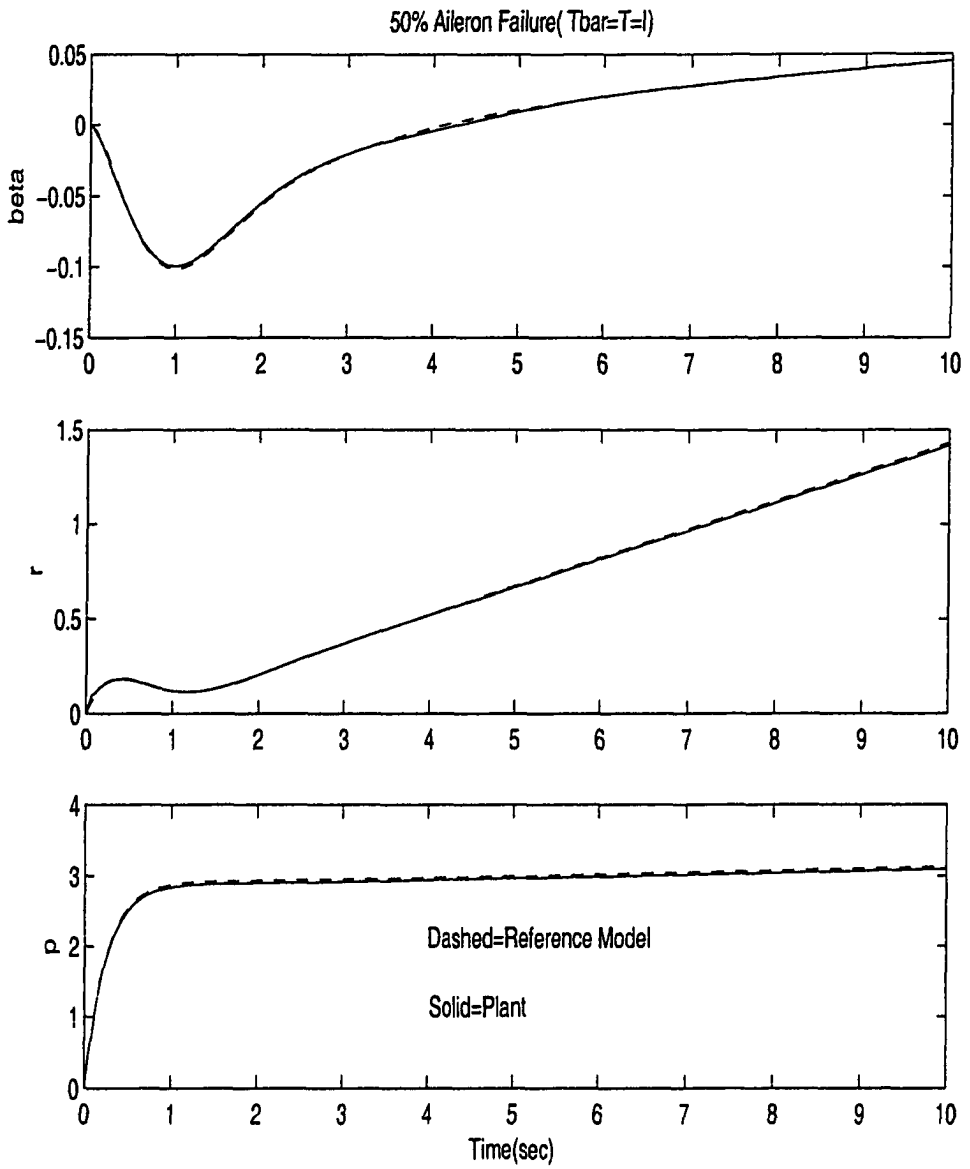

Figure 4.5: 50% Aileron Failure Using Adaptive Gains

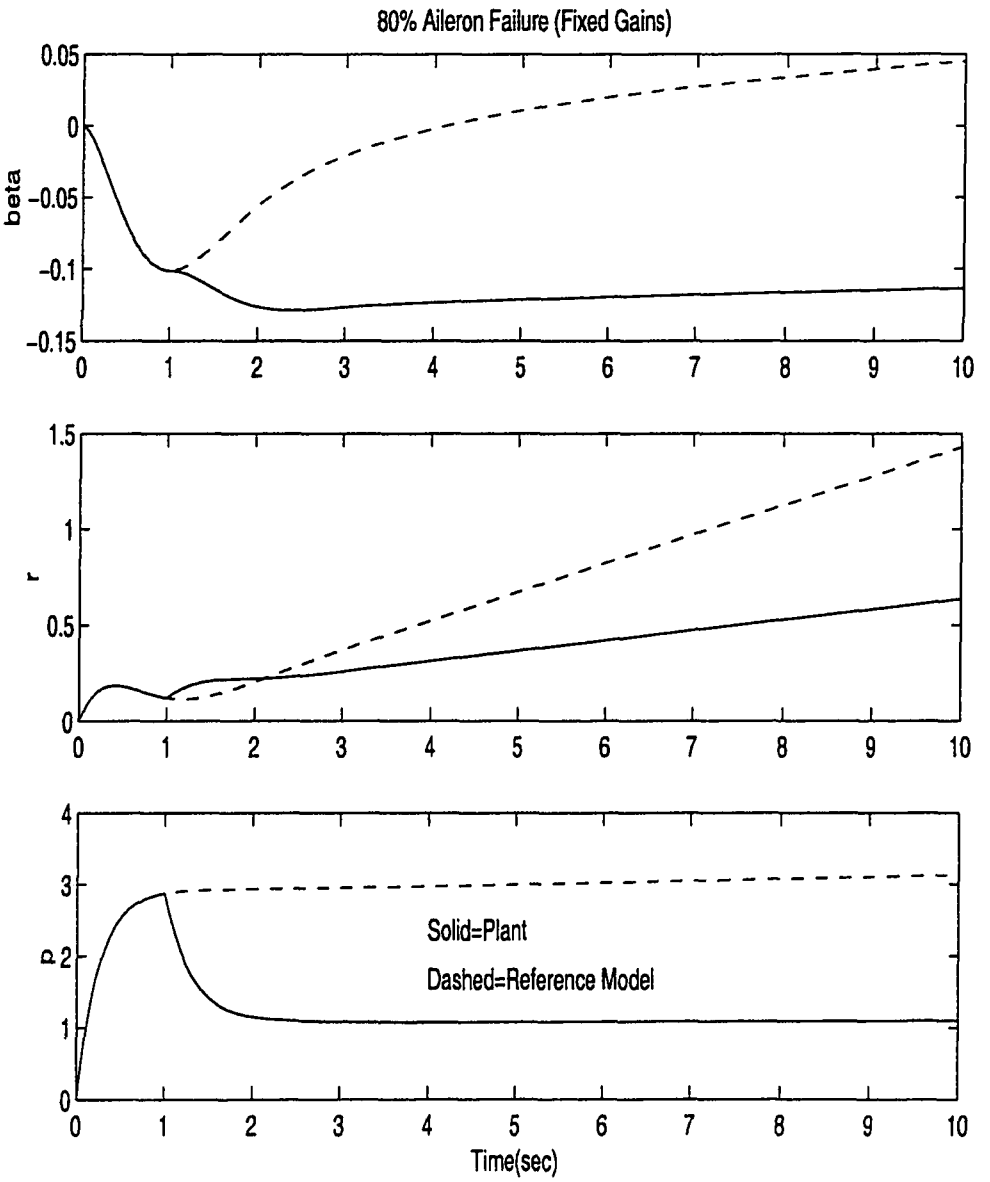

Figure 4.6: 80% Aileron Failure Using Fixed Gains

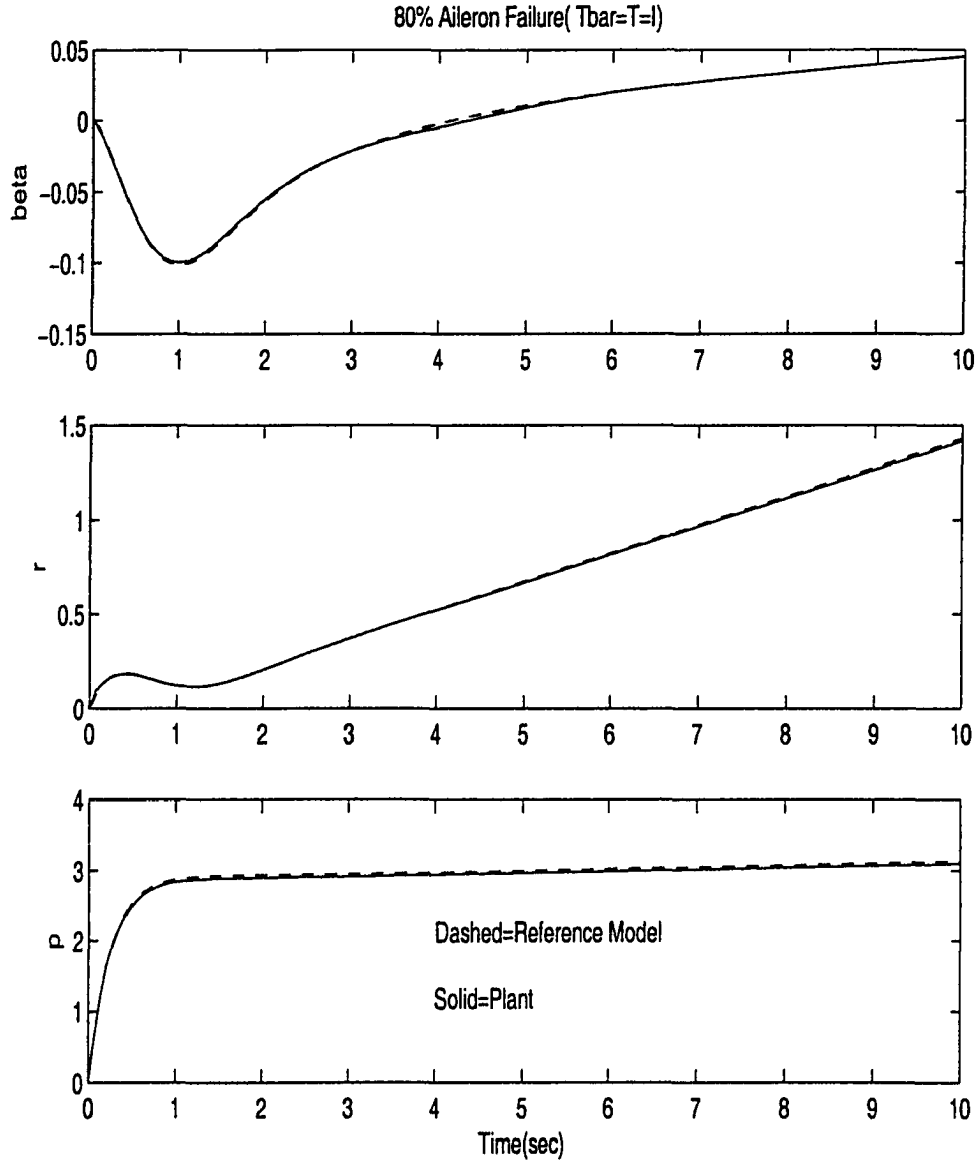

Figure 4.7: 80% Aileron Failure Using Adaptive Gains

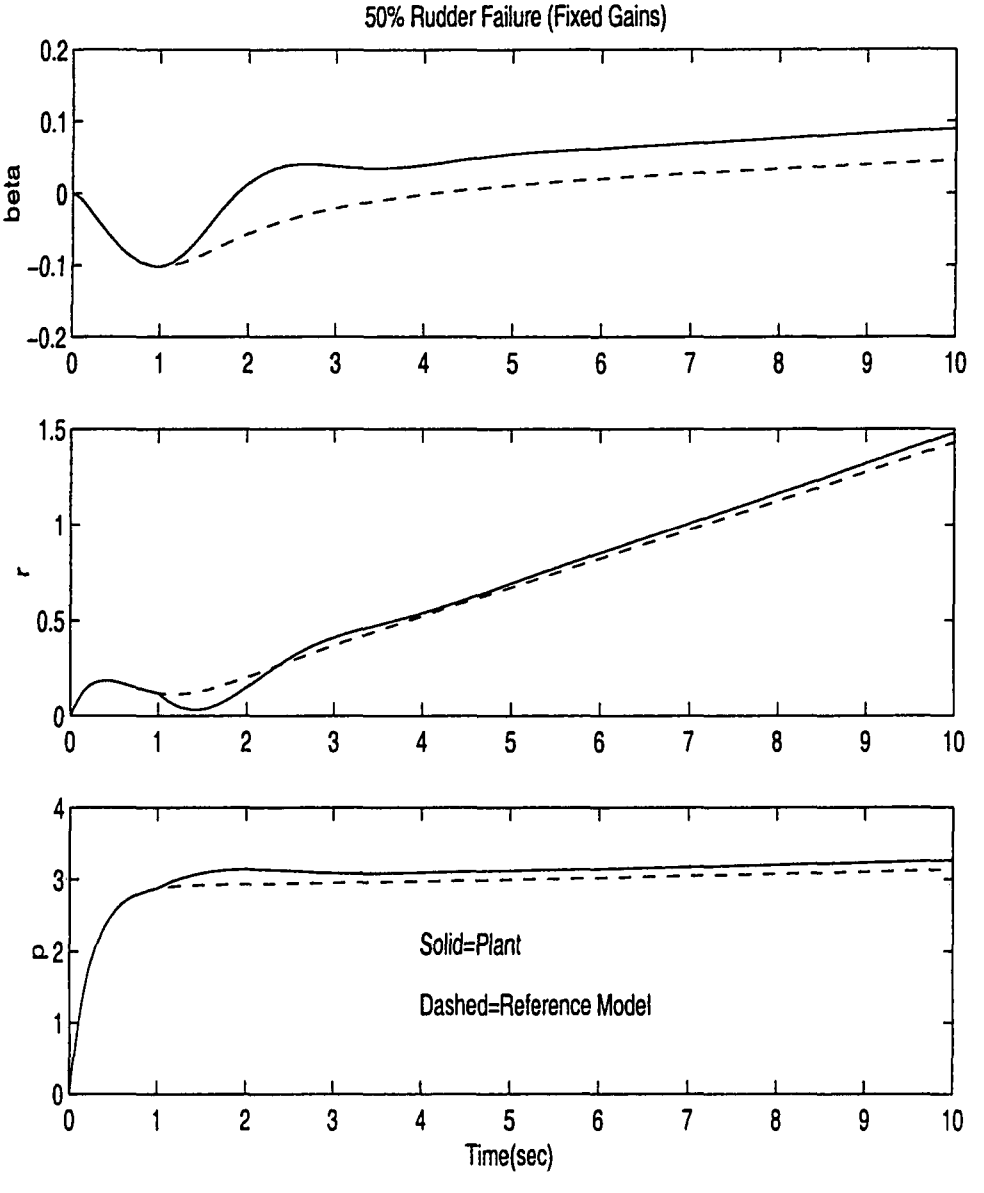

Figure 4.8: 50% Rudder Failure Using Fixed Gains

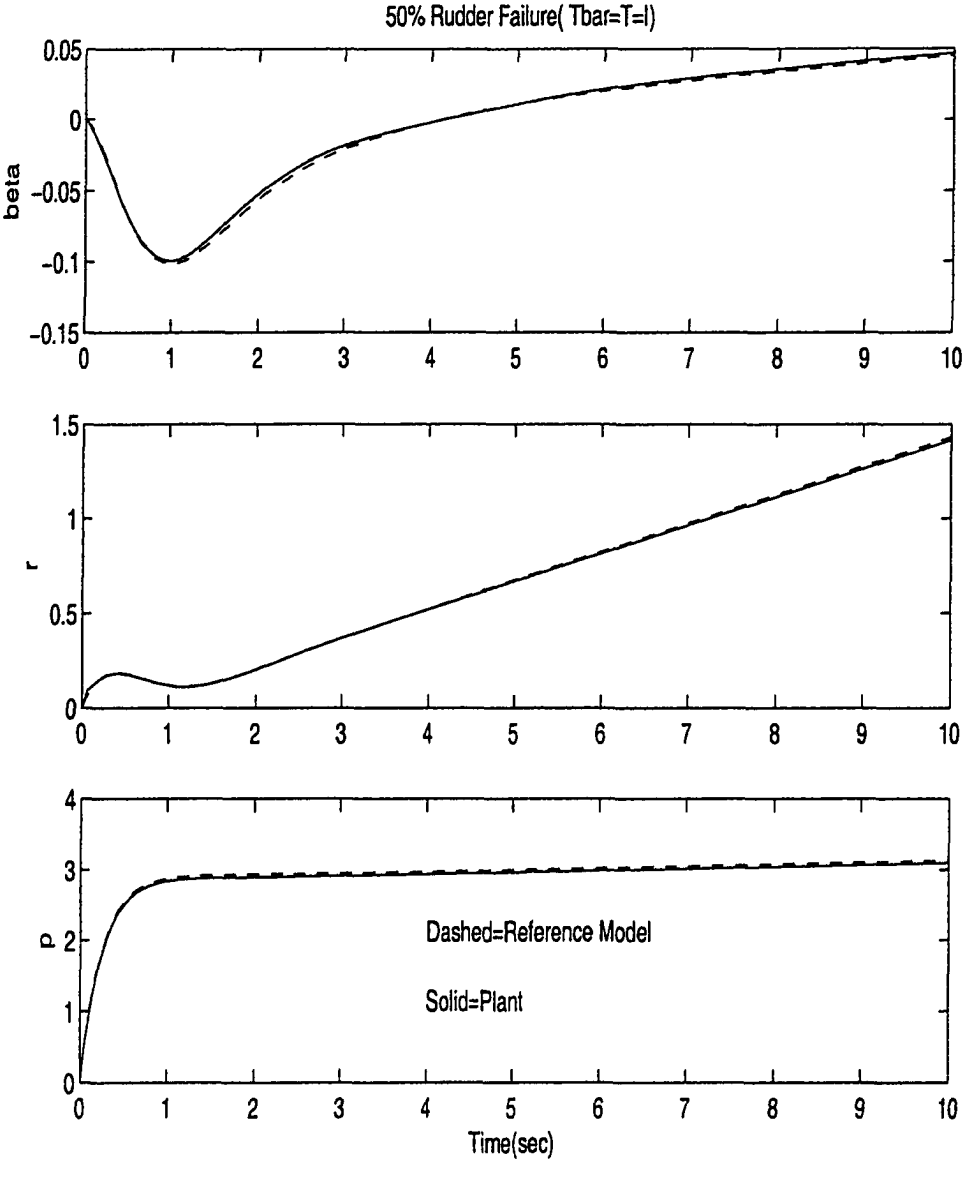

Figure 4.9: 50% Rudder Failure Using Adaptive Gains

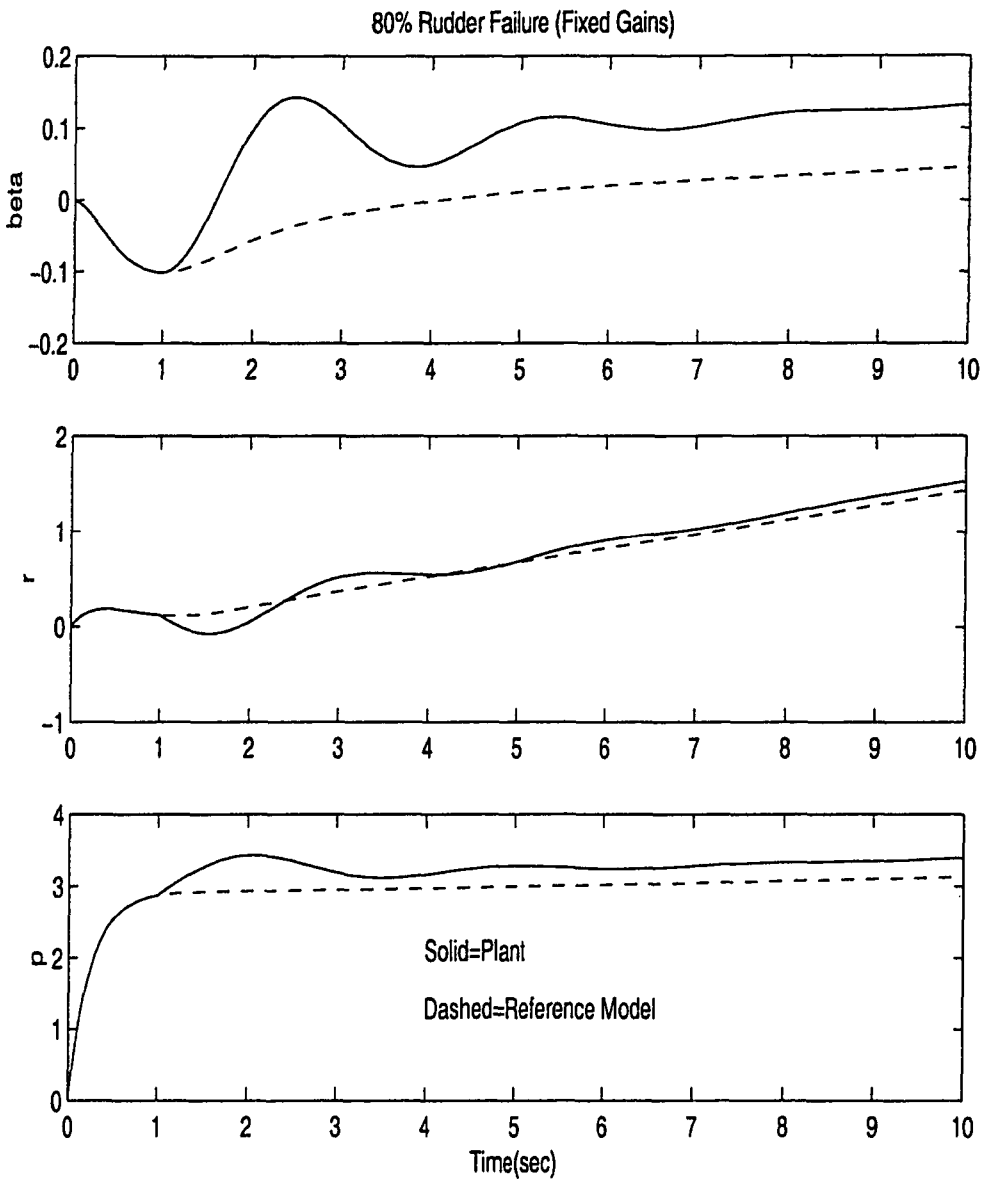

Figure 4.10: 80% Rudder Failure Using Fixed Gains

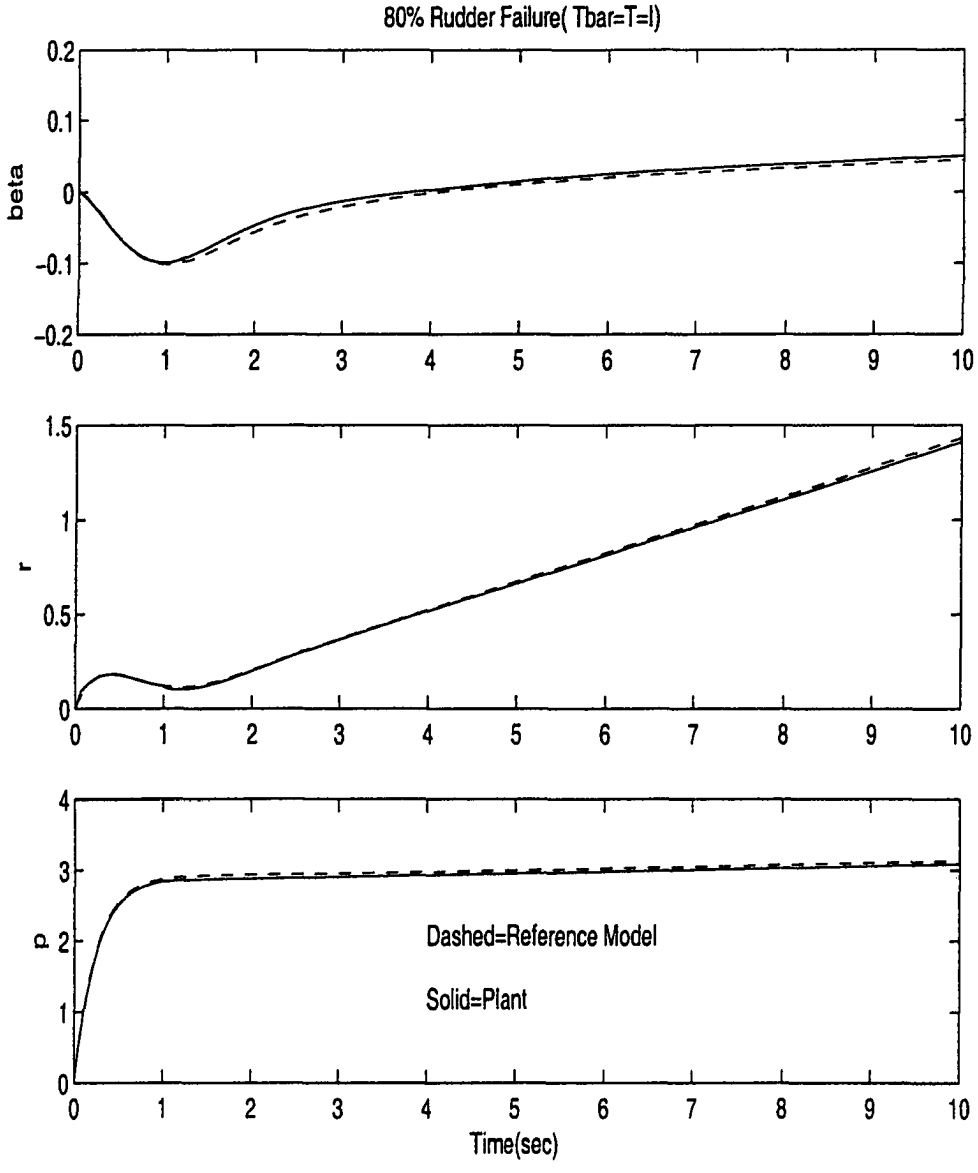

Figure 4.11: 80% Rudder Failure Using Adaptive Gains

Chapter 5

Concluding Remarks

5.1 Conclusions

This research has proposed new results for the design of passive and active fault tolerant control systems with application to aircraft flight control in the presence of aircraft control surface failures. The passive approach uses eigenstructure assignment and optimization to design fixed constant gain controllers. The active approach uses direct model reference adaptive control to adjust the controller gains in real time to maintain tracking when a failure occurs.

In chapter 2, one lemma and two theorems were proposed for eigenstruc-

ture invariance when it is known which control surface is most likely to fail. Lemma 2.1 derives a basis for the subspace in which the eigenvectors of the failed aircraft must lie. Theorem 2.1 shows the existence of a constant output feedback gain matrix which yields an invariant dominant eigenstructure both before and after failure. Theorem 2.2 shows that the failure of a control surface causes the corresponding row of the constant output feedback gain matrix to be zero. We applied our results to the design of a stability augmentation system for the linearized lateral dynamics of the F/A-18 aircraft. To achieve exact eigenstructure invariance, we required the dutch roll and the roll modes for both the unfailed and failed aircraft to be the same as for an eigenstructure assignment controller. The eigenstructure invariance was achieved but with increased coupling from sideslip to roll rate. To reduce the coupling, we required only the dutch roll for both the unfailed and failed aircraft to be the same as for the eigenstructure assignment controller. The coupling has been reduced but at the expense of exact eigenstructure invariance.

In chapter 3, we presented a passive fault tolerant flight control law for the F/A-18 aircraft which achieves acceptable handling qualities for a class of control surface failures. A comparison was made of an eigenstructure

assignment gain designed for the unfailed aircraft with a fault tolerant multiobjective gain. We have shown that the time responses for the unfailed aircraft using the eigenstructure assignment gain and the fault tolerant gain are identical. Furthermore, the passive fault tolerant controller achieves MIL-F-8785C specifications for all failure conditions.

In chapter 4, we presented a new result for direct adaptive control for multi-input multi-output systems with control surface failures. Two lemmas and one theorem were proposed for the stability of the adaptive closed loop system. Lemma 4.1 shows that positive definite quadratic Lyapunov functions can be selected such that their derivatives are negative semi definite. Lemma 4.2 shows the boundedness of these Lyapunov functions at the failure instants if the loss of control effectiveness failure does not exceed 50%. This condition has been shown via simulation to be only a sufficient condition. Theorem 4.1 proves the boundedness of all states and gains in the adaptive loop and that the augmented output error vanishes asymptotically.

We augmented the plant with a feedforward compensator such that the inverse feedforward compensator stabilizes the plant over the set of allowable failures. A novel state space approach for computing the feedforward

compensator was proposed. The approach uses the MATLAB® LMI Toolbox [14] and the MATLAB® Optimization Toolbox [15] to design a robust feedforward compensator.

We demonstrated the use of our algorithm by application to a three input model of the linearized lateral dynamics of the F/A-18 aircraft. We have presented simulation results which show that the adaptive controller exhibits improved model following as compared to a non-adaptive eigenstructure assignment controller.

The work of this thesis is documented in the following papers:

Belkharraz A.I., and Kenneth M. Sobel, *"Fault Tolerant Flight Control for a Class of Control Surface Failures "*. Proceedings of the American Control Conference, Chicago, Illinois. June 2000, pp 4209-4213.

Belkharraz A.I., and Kenneth M. Sobel, *"Eigenstructure Invariance for an Anticipated Flight Control Surface Failure"*, Proceedings of the American Control Conference , Arlington, VA June 2001, pp 1833-1835

Belkharraz A.I., and Kenneth M. Sobel, *"Direct Adaptive Control for Aircraft Control Surface Failures"*, Proceedings of the American Control Conference, Denver, CO June 2003, pp. 3905-3910.

Belkharraz A.I., and Kenneth M. Sobel, *"Direct Adaptive Control for Aircraft Control Surface Failures"*, submitted to International Journal of System Science.

5.2 Problems and Recommendations

We applied our design methodology to the linearized lateral dynamics of the F/A-18 aircraft. We computed an optimal constant feedback gain using an off-line multiobjective optimization technique. We observed that the response with the multiobjective optimization gain exhibits a significant coupling from sideslip to roll rate when a stabilator failure occurs. A possible extension will be the use of dynamic compensators which offer more degrees of freedom. Therefore, a dynamic controller may exist which reduces the coupling from sideslip to roll rate. This can be done by modeling the plant and the compensator by a composite system. A second order compensator can be tried first. If the desired dynamics are not achieved, then a

higher order compensator can be used. An important issue to be addressed is the choice of the subeigenvectors corresponding to the compensator.

The direct adaptive control algorithms using output feedback developed by Kaufman et. al. [12] have been extended to multi-input multi-output plants with control effectiveness failures. Our new adaptive algorithm has been applied to the linearized lateral dynamics of the F/A-18 aircraft in the presence of a loss of control effectiveness failure. Here the class of possible failures is the loss of control effectiveness of any one control surface. Furthermore, we do not know which control surface will fail nor do we know the amount of control effectiveness loss. However, if the class of control surface failures includes two or more simultaneous failures, then a single model based adaptive controller may be too slow to achieve an acceptable response. A possible extension will be the consideration of multiple models where each model will correspond to one control surface failure scenario which includes the multiple failure cases. The output of the plant is compared to the output of every model to determine the actual failure scenario. Then, we switch to the controller corresponding to this failure scenario. An important issue to be addressed is a proof of stability for the closed loop adaptive system.

Appendices

Appendix A

Proof of Lemma 2.1

$$(\lambda_i^d I - A_f) = \begin{bmatrix} (\lambda_i^d + \delta) I_m & 0_{m\times(n-m)} \\ -A_{21} + \Delta A_{21} & \lambda_i^d I - A_{22} \end{bmatrix} \tag{A.1}$$

$$(\lambda_i^d I - A_f)^{-1} = \frac{Adj(\lambda_i^d I - A_f)}{det(\lambda_i^d I - A_f)} \tag{A.2}$$

Let

$$(\lambda_i^d I - A_f) = A^i \tag{A.3}$$

Let $Adj(A^i) = [c_{pq}]^T$ where the cofactors c_{pq} are given by

$$c_{pq} = (-1)^{p+q} \cdot det(A^i_{pq}) \tag{A.4}$$

Due to the special structure of A^i, it follows that

$$c_{pq} = \begin{cases} (\lambda_i^d + \delta) \cdot det(A^i_{pq}) & \text{if } p = q,\ p,q = 1,2,\ldots,m \\ 0 & \text{if } p \neq q,\ p,q = 1,2,\ldots,m \end{cases} \tag{A.5}$$

Therefore, the adjoint of A^i may be written as

$$Adj(A^i) = \begin{bmatrix} (\lambda_i^d + \delta)\Gamma & (Adj(A^i))_{12} \\ (Adj(A^i))_{21} & (Adj(A^i))_{22} \end{bmatrix} \tag{A.6}$$

where $\Gamma = diag\{det(A^i_{11}), det(A^i_{22}), \ldots, det(A^i_{mm})\}$

Finally

$$\begin{aligned} (\lambda_i^d I - A_f)^{-1} B &= \frac{Adj(A^i) \cdot B}{det(A^i)} \\ &= \frac{1}{det(A^i)} \cdot \begin{bmatrix} (\lambda_i^d + \delta)\delta\Gamma \\ \delta(Adj(A^i))_{21} \end{bmatrix} \end{aligned} \tag{A.7}$$

Define

$$\alpha = \frac{(\lambda_i^d + \delta)\delta\Gamma}{det(A^i)} \tag{A.8}$$

$$\alpha_k = \frac{(\lambda_i^d + \delta)\delta det(A^i_{kk})}{det(A^i)}; \quad k = 1, \ldots, m$$

$$\gamma = \begin{bmatrix} \gamma_1, \ldots, \gamma_m \end{bmatrix} = \delta(Adj(A^i))_{21} \tag{A.9}$$

Then, the basis vectors are given by (2.11).

Appendix B

Proof of Theorem 2.1

$$\begin{aligned}(A_f + BFC)v_i^f &= (A + \Delta A + BFC)v_i^f \\ &= (A + BFC)v_i^f + \Delta A v_i^f \end{aligned} \tag{B.1}$$

Let the j^{th} control surface fail. Then

$$\Delta A v_i^f = \begin{bmatrix} & 0_m & & 0_{m\times(n-m)} \\ 0 \ \dots & a_{(m+1)j} & \dots \ 0 & \\ \vdots \ \dots & \vdots & \dots \ \vdots & 0_{(n-m)\times(n-m)} \\ 0 \ \dots & a_{nj} & \dots \ 0 & \end{bmatrix} \begin{bmatrix} v_{1i}^f \\ \vdots \\ v_{ni}^f \end{bmatrix} \tag{B.2}$$

From lemma 1, v_i^f may be written as

$$v_i^f = \beta_1 \begin{bmatrix} \alpha_1\delta \\ 0 \\ \vdots \\ 0 \\ \hline \\ \gamma_1 \end{bmatrix} + \ldots + \beta_j \begin{bmatrix} 0 \\ \vdots \\ 0 \\ \alpha_j\delta \\ 0 \\ \vdots \\ 0 \\ \hline \\ \gamma_j \end{bmatrix} + \ldots + \beta_m \begin{bmatrix} 0 \\ \vdots \\ 0 \\ \alpha_m\delta \\ \hline \\ \gamma_m \end{bmatrix} \tag{B.3}$$

Observe that all the basis vectors have a zero in row j with the exception of basis vector j.

Choose $\beta_j = 0$. Then, $\Delta A v_i^f = 0$ and (2.16) is proven.

Appendix C

Proof of Theorem 2.2

Rewriting the eigenvalue-eigenvector equation we obtain

$$(\lambda_i I - A_f)v_i^f = BFCv_i^f \tag{C.1}$$

We partition (C.1) conformally mindful of the special structure of A_f and B.

Let

$$v_i^f = \begin{bmatrix} z_i \\ w_i \end{bmatrix} \tag{C.2}$$

Then, Eq. (C.1) may be rewritten as

$$\begin{bmatrix} (\lambda_i + \delta)I_m & 0_{m\times(n-m)} \\ -A_{21} + \Delta A_{21} & \lambda_i I_{(n-m)} - A_{22} \end{bmatrix} \begin{bmatrix} z_i \\ w_i \end{bmatrix} = \delta \begin{bmatrix} I_m \\ 0_{(n-m)\times m} \end{bmatrix} FC \begin{bmatrix} z_i \\ w_i \end{bmatrix}$$

Considering the first matrix equation from the partitioned form, we obtain

$$\begin{bmatrix} (\lambda_i+\delta)I_m & 0_{m\times(n-m)} \end{bmatrix} \begin{bmatrix} z_i \\ w_i \end{bmatrix} = \delta \begin{bmatrix} I_m \\ 0_{m\times(n-m)} \end{bmatrix} FC \begin{bmatrix} z_i \\ w_i \end{bmatrix}$$

$$= \delta FC \begin{bmatrix} z_i \\ w_i \end{bmatrix} \tag{C.3}$$

$$(\lambda_i+\delta)I_m z_i = \delta FC v_i^f;\ i=1,\ldots,r \tag{C.4}$$

Thus

$$(\frac{\lambda_i+\delta}{\delta})z_i = FCv_i^f;\ i=1,\ldots,r \tag{C.5}$$

Let

$$Z = \begin{bmatrix} (\frac{\lambda_1+\delta}{\delta})z_1, & (\frac{\lambda_2+\delta}{\delta})z_2, & \ldots, & (\frac{\lambda_r+\delta}{\delta})z_r \end{bmatrix} \tag{C.6}$$

$$V_f = \begin{bmatrix} v_1^f, & v_2^f, & \ldots, & v_r^f \end{bmatrix} \tag{C.7}$$

Therefore

$$Z = FCV_f \tag{C.8}$$

and

$$F = Z(CV_f)^{-1} \tag{C.9}$$

Finally,

$$z_i = \begin{bmatrix} x \\ \vdots \\ x \\ 0 \\ x \\ \vdots \\ x \end{bmatrix} \quad \textit{where the zero is in row } j;\ j \leq m \tag{C.10}$$

So

$$F = \begin{bmatrix} & \vdots & \\ 0 & 0 \ \ldots \ 0 & \\ & \vdots & \end{bmatrix} (CV_f)^{-1} \tag{C.11}$$

where the zeros are in row j of matrix F. Then, the result follows.

Appendix D

Derivation of Error Equation

Define $e_x = x_p^* - x_p^a$. Then,

$$\dot{e}_x = \dot{x}_p^* - \dot{x}_p^a \tag{D.1}$$

Add and substract $A_p^a x_p^*$ in Equation (D.1) and obtain:

$$\dot{e}_x = \dot{x}_p^* - A_p^a x_p^* + A_p^a x_p^* - \dot{x}_p^a \tag{D.2}$$

$$\dot{e}_x = S_{11}A_m x_m + S_{11}B_m u_m + S_{12}\dot{u}_m - A_p^a x_p^* + A_p^a x_p^* - A_p^a x_p^a - B_p^a \alpha^i u_p \tag{D.3}$$

Recall that

$u_p = K_r r$, where $K_r = K_I + K_p$ and $r = [(e_y^a)^T \; x_m^T \; u_m^T]^T$

From Eq. (4.13) we have

$$x_p^* = S_{11}x_m + S_{12}u_m \tag{D.4}$$

Hence

$$\begin{aligned}\dot{e}_x &= A_p^a e_x - B_p^a \alpha^i K_r r + S_{11} A_m x_m + S_{11} B_m u_m + \\ &\quad S_{12} \dot{u}_m - A_p^a S_{11} x_m - A_p^a S_{12} u_m \qquad \text{(D.5)}\end{aligned}$$

$$\begin{aligned}\dot{e}_x &= A_p^a e_x - B_p^a \alpha^i K_r r + (S_{11} A_m - A_p^a S_{11}) x_m + \\ &\quad (S_{11} B_m - A_p^a S_{12}) u_m \qquad \text{(D.6)}\end{aligned}$$

add and substract $B_p^a \alpha^i \tilde{K}_i r$ in (D.6), where $\tilde{K}_i = [\tilde{K}_{ei}, \tilde{K}_{xi}, \tilde{K}_{ui}]$

$$\begin{aligned}\dot{e}_x &= A_p^a e_x - B_p^a \alpha^i K_r r + B_p^a \alpha^i \tilde{K}_i r + (S_{11} A_m - A_p^a S_{11}) x_m + \\ &\quad (S_{11} B_m - A_p^a S_{12}) u_m - B_p^a \alpha^i \tilde{K}_{ei} e_y^a - \\ &\quad B_p^a \alpha^i \tilde{K}_{xi} x_m - B_p^a \alpha^i \tilde{K}_{ui} u_m \qquad \text{(D.7)}\end{aligned}$$

Define the augmented output tracking error as

$$e_y^a = y_m - y_p^a = y^* - y_p^a = C_p^a x_p^* - C_p^a x_p^a = C_p^a e_x$$

$$\begin{aligned}\dot{e}_x &= (A_p^a - B_p^a \alpha^i \tilde{K}_{ei} C_p^a) e_x + (S_{11} A_m - A_p^a S_{11} - B_p^a \alpha^i \tilde{K}_{xi}) x_m - \\ &\quad B_p^a \alpha^i [K_r - \tilde{K}_i] r + (S_{11} B_m - A_p^a S_{12} - B_p^a \alpha^i \tilde{K}_{ui}) u_m \qquad \text{(D.8)}\end{aligned}$$

Let $\tilde{K}_{xi} = S_{21}$; $\tilde{K}_{ui} = S_{22}$; $\tilde{K}_{ui} = S_{23}$, and define $A_c = A_p^a - B_p^a \alpha^i \tilde{K}_{ei} C_p^a$

$$\begin{aligned}\dot{e}_x &= A_c e_x - B_p^a \alpha^i [K_r - \tilde{K}_i] r + [S_{11} A_m - A_p^a S_{11} - B_p^a \alpha^i S_{21}] x_m + \\ &\quad (S_{11} B_m - A_p^a S_{12} - B_p^a \alpha^i S_{22}) u_m \qquad \text{(D.9)}\end{aligned}$$

Since $q \leq m$, use Eq. (4.20) to obtain

$$\dot{e}_x = A_c e_x - B_p^a \alpha^i [K_r - \tilde{K}_i] r \tag{D.10}$$

Appendix E

Proof of Lemma 4.1

Consider the Lyapunov function:

$$V_i(e_x, K_I) = e_x^T P_i e_x + tr[(K_I - \tilde{K}_i)T^{-1}(K_I - \tilde{K}_i)^T] \tag{E.1}$$

where P_i is an $n \times n$ postive definite symmetric matrix, $\tilde{K}_i$ is an unspecified matrix, T^{-1} is a positive definite matrix, and, "tr" denotes the trace. Note that V_i is positive definite in the state variables of the adaptive system, $e_x(t)$ and $K_I(t)$.

The time derivative of V_i is

$$\begin{aligned} \dot{V}_i &= \dot{e}_x^T P_i e_x + e_x^T P_i \dot{e}_x + tr[\dot{K}_I T^{-1}(K_I - \tilde{K}_i)^T + \\ &\quad (K_I - \tilde{K}_i)T^{-1}\dot{K}_I^T] \qquad \text{(E.2)} \\ \dot{V}_i &= \dot{e}_x^T P_i e_x + e_x^T P_i \dot{e}_x + 2tr[(K_I - \tilde{K}_i)T^{-1}\dot{K}_I^T] \qquad \text{(E.3)} \end{aligned}$$

Use Eqs. (4.25)-(4.29) to obtain

$$\begin{aligned}
\dot{V}_i &= [A_c e_x - B_p^a \alpha^i [K_r - \tilde{K}_i] r]^T P_i e_x + \\
&\quad e_x^T P_i [A_c e_x - B_p^a \alpha^i [K_r - \tilde{K}_i] r] + \\
&\quad 2tr[(K_I - \tilde{K}_i) T^{-1} Tr(e_y^a)^T] \qquad \text{(E.4)} \\
\dot{V}_i &= e_x^T A_c^T P_i e_x + e_x^T P_i A_c e_x - [B_p^a \alpha^i (K_r - \tilde{K}_i) r]^T P_i e_x - \\
&\quad e_x^T P_i B_p^a \alpha^i (K_r - \tilde{K}_i) r + 2(e_y^a)^T (K_I - \tilde{K}_i) r \qquad \text{(E.5)} \\
\dot{V}_i &= e_x^T (A_c^T P_i + P_i A_c) e_x - 2 e_x^T P_i B_p^a \alpha^i (K_r - \tilde{K}_i) r + \\
&\quad 2 e_x^T (C_p^a)^T K_I r - 2 e_x^T (C_p^a)^T \tilde{K}_i r \qquad \text{(E.6)} \\
\dot{V}_i &= e_x^T (A_c^T P_i + P_i A_c) e_x - 2 e_x^T P_i B_p^a \alpha^i K_r r + \\
&\quad 2 e_x^T P_i B_p^a \alpha^i \tilde{K}_i r + 2 e_x^T (C_p^a)^T K_I r - 2 e_x^T (C_p^a)^T \tilde{K}_i r \qquad \text{(E.7)} \\
\dot{V}_i &= e_x^T (A_c^T P_i + P_i A_c) e_x - 2 e_x^T P_i B_p^a \alpha^i (K_I + K_p) r + \\
&\quad 2 e_x^T P_i B_p^a \alpha^i \tilde{K}_i r + 2 e_x^T (C_p^a)^T K_I r - 2 e_x^T (C_p^a)^T \tilde{K}_i r \qquad \text{(E.8)} \\
\dot{V}_i &= e_x^T (A_c^T P_i + P_i A_c) e_x - 2 e_x^T P_i B_p^a \alpha^i K_I r - 2 e_x^T P_i B_p^a \alpha^i K_p r + \\
&\quad 2 e_x^T P_i B_p^a \alpha^i \tilde{K}_i r + 2 e_x^T (C_p^a)^T K_I r - 2 e_x^T (C_p^a)^T \tilde{K}_i r \qquad \text{(E.9)}
\end{aligned}$$

Let $(C_p^a)^T = P_i B_p^a \alpha^i$. Then, the time derivative of V_i becomes

$$\dot{V}_i = e_x^T (A_c^T P_i + P_i A_c) e_x - 2 e_x^T P_i B_p^a \alpha^i K_p r \qquad \text{(E.10)}$$

Substitute for K_p from Eq. (4.26) and recall $(C_p^a)^T = P_i B_p^a \alpha^i$ to obtain

$$\dot{V}_i = e_x^T (A_c^T P_i + P_i A_c) e_x - 2 e_x^T (C_p^a)^T e_y^a r^T \bar{T} r \qquad \text{(E.11)}$$

$$\dot{V}_i = e_x^T (A_c^T P_i + P_i A_c) e_x - 2(e_y^a)^T e_y^a r^T \bar{T} r \tag{E.12}$$

$$\dot{V}_i = -e_x^T Q_i e_x - 2(e_y^a)^T e_y^a r^T \bar{T} r \leq 0 \qquad t \in (T_i, T_{i+1}) \tag{E.13}$$

where $Q_i = -(A_c^T P_i + P_i A_c)$

Appendix F

Proof of Lemma 4.2

To prove the boundedness of $V_i(t)$ at the failure times T_i, we will begin with $V_0(t)$ which is bounded. At the first failure time we switch to $V_1(t)$ which will be proven to be bounded at T_1.

$$V_0(t) = e_x^T P_0 e_x + tr[(K_I - \tilde{K}_0)T^{-1}(K_I - \tilde{K}_0)^T] \quad for \quad t \in [0,\infty) \quad \text{(F.1)}$$

When the first failure occurs at time T_1, we will switch to $V_1(t)$

$$V_1(t) = e_x^T P_1 e_x + tr[(K_I - \tilde{K}_1)T^{-1}(K_I - \tilde{K}_1)^T] \quad for \quad t \in [0,\infty) \quad \text{(F.2)}$$

Recall that

$$\dot{V}_0 = -e_x^T Q_0 e_x - 2(e_y^a)^T e_y^a r^T \bar{T} r \quad for\ t \in [0, T_1) \quad \text{(F.3)}$$

$$\dot{V}_1 = -e_x^T Q_1 e_x - 2(e_y^a)^T e_y^a r^T \bar{T} r \quad for\ t \in (T_1, T_2) \quad \text{(F.4)}$$

where T_2 is the instant of the second failure.

Observe that $\dot{V}_0 < 0$, and $\dot{V}_1 < 0$ .Therefore $V_0(t)$ and $V_1(t)$ are bounded monotone nonincreasing functions on $t \in [0, T_1)$ and $t \in (T_1, T_2)$ respectively. Therefore

$$V_0(0) \geq V_0(T_1) \tag{F.5}$$

$$V_1(T_1) \geq V_1(T_2) \tag{F.6}$$

For the purpose of the proof we will use the following.

Lemma F.1 *For any real constant square matrices, we have*

$tr[(A-B)T^{-1}(A-B)^T] \leq 2tr(AT^{-1}A^T) + 2tr(BT^{-1}B^T)$

where T^{-1} is positive definite symmetric.

Proof: See Appendix I.

Let $A = K_I - \tilde{K}_0$, and $B = \tilde{K}_1 - \tilde{K}_0$. Use Lemma F.1 to obtain

$$tr[(K_I - \tilde{K}_1)T^{-1}(K_I - \tilde{K}_1)^T] \leq 2tr[(K_I - \tilde{K}_0)T^{-1}(K_I - \tilde{K}_0)^T] + 2tr[(\tilde{K}_1 - \tilde{K}_0)T^{-1}(\tilde{K}_1 - \tilde{K}_0)^T]$$

Define $\Delta V_1 = tr[(\tilde{K}_1 - \tilde{K}_0)T^{-1}(\tilde{K}_1 - \tilde{K}_0)^T] = constant$, then

$$tr[(K_I - \tilde{K}_1)T^{-1}(K_I - \tilde{K}_1)^T] \leq 2tr[(K_I - \tilde{K}_0)T^{-1}(K_I - \tilde{K}_0)^T] + 2\Delta V_1$$

$$V_1(T_1) - e_x^T P_1 e_x \leq 2V_0(T_1) - 2e_x^T P_0 e_x + 2\Delta V_1 \tag{F.7}$$

$$V_1(T_1) \leq 2V_0(T_1) + e_x^T P_1 e_x - 2e_x^T P_0 e_x + 2\Delta V_1 \quad \text{(F.8)}$$

$$V_1(T_1) \leq 2V_0(T_1) + e_x^T (P_1 - 2P_0) e_x + 2\Delta V_1 \quad \text{(F.9)}$$

From Eq. (F.5) we have $V_0(0) \geq V_0(T_1)$, and therefore

$$V_1(T_1) \leq 2V_0(0) + e_x^T (P_1 - 2P_0) e_x + 2\Delta V_1 \quad \text{(F.10)}$$

Since $V_0(0)$ is bounded, and ΔV_1 is a constant, then $(P_1 - 2P_0)$ has to be at least negative semidefinite.

From the ASPR condition we have

$$(C_p^a)^T = P_0 B_p^a \quad \text{(F.11)}$$

$$(C_p^a)^T = P_1 B_p^a \alpha^1 \quad \text{(F.12)}$$

This implies that

$$P_0 B_p^a = P_1 B_p^a \alpha^1 \quad \text{(F.13)}$$

By premultiplying both sides of (F.13) by $(B_p^a)^T$ we obtain

$$(B_p^a)^T P_0 B_p^a = (B_p^a)^T P_1 B_p^a \alpha^1 \quad \text{(F.14)}$$

Lemma F.2 *[26] If $P_0 \in \Re^{n \times n}$ is positive definite and $B \in \Re^{n \times m}$ has rank m then*

$$N_0 = B^T P_0 B$$

is also positive definite.

Since P_0 and P_1 are positive definite, then by applying Lemma F.2, we obtain

$$N_0 = N_1 \alpha^1 \tag{F.15}$$

where N_0 and N_1 are also positive definite.

We present several results on congruence transformation.

Definition F.1 *[27]: If there exists a nonsingular matrix S such that $B = S^H AS$ we say that B is hermitian-congruent to A, and that B is obtained from A by a hermitian congruence transformation.*

Lemma F.3 *[27]: If $x^H Ax$ is a positive definite quadratic form and $B = S^H AS$, where S is a nonsingular square matrix, then $x^H Bx$ is also a positive definite quadratic form. Similarly for positive semidefinite forms, etc.*

Lemma F.3 shows that the property of being positive definite is not affected by a congruence transformation. To show the boundedness one needs to show that $(P_1 - 2P_0)$ is at least negative semi-definite. This is equivalent to showing that $(N_1 - 2N_0)$, or $(N_1 - 2N_1\alpha^1)$ is at least negative semi-definite. To complete the proof we will use the following lemma.

Lemma F.4 *[28]: If A and B are symmetric matrices and A is positive definite, there exists a nonsingular matrix S, such that*

$$S^T(A+B)S = I+G$$

where G is a diagonal matrix whose elements are eigenvalues of $A^{-1}B$.

According to lemma F.4 there exists a nonsingular matrix S such that

$$S^T(N_1 - 2N_1\alpha^1)S = I+G \tag{F.16}$$

where $G = diag\{\lambda_i(N_1^{-1}(-2N_1\alpha^1))\} = -2diag\{\lambda_i(\alpha^1)\} = -2diag\{\alpha_k^1\}$, which implies

$$S^T(N_1 - 2N_1\alpha^1)S = I - 2diag\{\alpha_k^1\} \tag{F.17}$$

Observe that according to Definition F.1, $(N_1 - 2N_1\alpha^1)$ and $(I - 2diag\{\alpha_k^1\})$ are related by a congruence relationship. Hence, the positive or negative definiteness property of these two matrices is the same. Finally, we have: If $\alpha_k^1 \geq \frac{1}{2}$, then $\lambda_i(I - 2diag\{\alpha_k^1\})$ are all negative, and $(I - 2diag\{\alpha_k^1\})$ is negative semi definite. Since $(I - 2diag\{\alpha_k^1\})$ is congruent to $(N_1 - 2N_1\alpha^1)$, then $(N_1 - 2N_1\alpha^1)$ and hence $(P_1 - 2P_0)$ are also negative semidefinite. From Eq. (F.10) and using $e_x^T(P_1 - 2P_0)e_x \leq 0$ yields

$$V_1(T_1) \leq 2V_0(0) + e_x^T(P_1 - 2P_0)e_x + 2\Delta V_1 \leq 2V_0(0) + 2\Delta V_1 \tag{F.18}$$

In the same manner, generally:

$$V_i(t) \leq V_i(T_i) \leq \gamma V_{i-1}(T_i) + \delta \leq \ldots \leq \eta V_0(0) + \beta \tag{F.19}$$

where γ, δ, η, and β are constant real numbers.

Appendix G

Proof of Theorem 4.1

We show that $e_x \to 0$ as $t \to \infty$ by using the following Lemma.

Lemma G.1 *[29]*

If $f, \dot{f} \in L_\infty$ *and* $f \in L_p$ *for some* $p \in [1, \infty)$ *then* $f(t) \to 0$ *as* $t \to \infty$

Consider the interval (T_{q0}, ∞). It follows from (E.13) that

$$\dot{V}_{q0} \leq -k\|e_x\|^2; \quad k > 0 \tag{G.1}$$

Therefore, V_{q0} is a bounded nonincreasing function. So it has a limit as $t \to \infty$ which we denote by V_∞. Furthermore, K_I and e_x are also bounded, i.e., $e_x \in L_\infty$. From (D.10), we observe that since A_c is stable, and e_x, K_I, x_m, u_m are bounded, then $\dot{e}_x$ is also bounded, i.e., $\dot{e}_x \in L_\infty$.

We integrate both sides of (G.1) to obtain

$$\begin{aligned} \int_0^\infty \dot{V}_{q_0} dt &\leq -k \int_0^\infty \|e_x\|^2 dt \\ \int_0^\infty \|e_x\|^2 dt &\leq \frac{-1}{k} \int_0^\infty \dot{V}_{q_0} dt = \frac{1}{k} \int_\infty^0 \dot{V}_{q_0} dt = \frac{V(0) - V_\infty}{k} < \infty \end{aligned}$$

Therefore, $e_x \in L_2$.

Since $e_x, \dot{e}_x \in L_\infty$ and $e_x \in L_2$, then it follows from Lemma G.1 that $e_x \to 0$ as $t \to \infty$.

Appendix H

Proof of Theorem 4.2

The system in (4.35) with feedback $H(s) = K(1+\tau s)$ is given by

$$\dot{x} = A_{cl}^{j}(\sigma)x \tag{H.1}$$

where

$$A_{cl}^{j}(\sigma) = A_p - B_p^j(\sigma)[I+\tau KC_pB_p^j(\sigma)]^{-1}KC_p(I+\tau A_p) \tag{H.2}$$

A necessary and sufficient condition for the existence of the inverse in (H.2) is that the eigenvalues λ_i satisfy

$$1+\tau\lambda_i\{KC_pB_p^j(\sigma)\} \neq 0 \tag{H.3}$$

Use the matrix inversion lemma to obtain

$$A_{cl}^{j}(\sigma) = A_p - B_p^j(\sigma)[I-\tau KC_p(I+\tau B_p^j(\sigma)KC_p)^{-1}B_p^j(\sigma)]KC_p(I+\tau A_p) \tag{H.4}$$

Rearrange (H.4) to obtain

$$A_{cl}^{j}(\sigma) = (A_p - B_p^j(\sigma)KC_p) + [\tau B_p^j(\sigma)KC_p(I+\tau B_p^j(\sigma)KC_p)^{-1}B_p^j(\sigma)KC_p(I+\tau A_p) - B_p^j(\sigma)KC_p\tau A_p] \quad \text{(H.5)}$$

where K is computed so that $(A_p - B_p^j(\sigma)KC_p)$ is stable for all j and σ.

Use the result from Sobel et. al. [30] that the system in (H.1) is stable if

$$\alpha > K_2(M)\beta \quad \text{(H.6)}$$

where

$$\alpha = -max\, Re[\lambda_i(A_p - B_p^j(\sigma)KC_p)] \quad \text{(H.7)}$$

$K_2(M)$ is the condition number of the modal matrix of $(A_p - B_p^j(\sigma)KC_p)$.

and

$$\|\tau B_p^j(\sigma)KC_p(I+\tau B_p^j(\sigma)KC_p)^{-1}B_p^j(\sigma)KC_p(I+\tau A_p) - B_p^j(\sigma)KC_p\tau A_p\| \leq \beta \quad \text{(H.8)}$$

It is clear that β can be made small by choosing τ sufficiently small.

Let α_{min} be the minimum of α over j, σ; and let $K_{2_{max}}$ be the maximum of $K_2(M)$ over j, σ.

Then, we require

$$\beta < \alpha_{min}/K_{2_{max}} \quad \text{(H.9)}$$

Hence, there exists τ sufficiently small such that (H.9) is satisfied which implies that $A_{cl}^{j}(\sigma)$ in (H.4) is a stability matrix for all j, σ.

Appendix I

Proof of Lemma F.1

$tr[(A-B)T^{-1}(A-B)^T] \leq 2tr(AT^{-1}A^T)+2tr(BT^{-1}B^T)$ is true if

$$2tr(AT^{-1}A^T)+2tr(BT^{-1}B^T)-tr[(A-B)T^{-1}(A-B)^T] \geq 0 \qquad \text{(I.1)}$$

$$\begin{aligned}
LHS\ of\ Eq.\ (\text{I.1}) &= 2tr(AT^{-1}A^T)+2tr(BT^{-1}B^T)- \\
&\quad tr[AT^{-1}A^T-AT^{-1}B^T-BT^{-1}A^T+BT^{-1}B^T] \\
&= 2tr(AT^{-1}A^T+BT^{-1}B^T)- \\
&\quad tr[AT^{-1}A^T-AT^{-1}B^T-BT^{-1}A^T+BT^{-1}B^T] \\
&= tr[2AT^{-1}A^T+2BT^{-1}B^T-AT^{-1}A^T+ \\
&\quad AT^{-1}B^T+BT^{-1}A^T-BT^{-1}B^T] \\
&= tr[AT^{-1}A^T+AT^{-1}B^T+BT^{-1}A^T+BT^{-1}B^T] \\
&= tr[(A+B)T^{-1}(A+B)^T] \geq 0
\end{aligned}$$

Bibliography

[1] Gavito, V.F., and Collins, D.J., "Application of eigenstructure assignment to self reconfiguring aircraft MIMO controllers," *AIAA Paper 87–2235.*

[2] Napolitano, M.R., and Swaim, R.L., "Redesign of the feedback structure following a battle damage and/or a failure on a control surface by eigenstructure assignment," *AIAA Paper 91–2626–CP.*

[3] Jiang, J., "Design of reconfigurable control systems using eigenstructure assignment," *International Journal of Control,* Vol. 59, No. 2, pp. 395-410, 1994.

[4] Jiang, J., and Zhao, Q., "Design of Reliable Control Systems Possessing Actuator Redundancies" *J. of Guidance ,Control, and Dynamics,* Vol. 23, No. 4, July-August 2000.

[5] Gorrec, Y.L., Magni, J.F., and Chiapp, C., "Modal Multimodel Control Design Approach Applied to Aircraft Autopilot Design" *J. of Guidance ,Control, and Dynamics,* Vol. 21, No. 1, January-February 1998.

[6] Boskovic, J.D., and Mehra, R.K., "A Stable Scheme for Automatic Control Reconfiguration in the Presence of Actuator Failures" *Proceedings of the American Control Conference,* Vol.4, pp. 2455-2459, 1998.

[7] Boskovic, J.D., and Mehra, R.K., "A Multiple Model-based Reconfigurable Control System Design" *Proceedings of 37th IEEE Confernce on Decision and Control,* Tampa, Florida, December 1998.

[8] Boskovic, J.D., and Mehra, R.K., "Intelligent Adaptive Control of a Tailless Advanced Fighter Aircraft Under Wing Damage" *J. of Guidance ,Control, and Dynamics,* Vol. 23, No. 5, September-October 2000.

[9] Boskovic, J.D., and Mehra, R.K., "Multiple-Model Adaptive Flight Control Scheme for Accomodation of Actuator Failures" *J. of Guidance ,Control, and Dynamics,* Vol. 25, No. 4, pp. 712-724 July-August 2002.

[10] Tao, G., Ma, X., and Joshi, S.M., "Adaptive State Feedback and Tracking Control of Systems with Actuator Failures" *IEEE Transactions on Automatic Control,* Vol. 46, No. 1, pp. 78-94, Jan. 2001.

[11] Tao, G., Shuhao, C., and Joshi, S.M., "An Adaptive Actuator Failure Compensation Controller Using Output Feedback" *IEEE Transactions on Automatic Control,* Vol. 47, No. 3, pp.506-511, March 2002

[12] Kaufman, H., Barkana, I., and Sobel, K.M., "Direct Adaptive Control Algorithms: Theory and Applications", Second Edition, *Springer-Verlag New York, Inc.*, 1998.

[13] Morse, W.D., and Ossman, K.A., "Model Following Reconfigurable Flight Control System for the AFTI/F-16" *J. of Guidance ,Control, and Dynamics,* Vol. 13, No. 6, November-December 1990.

[14] Pascal, G., Arkadi, N., Alan, L., Mahmoud, C., "LMI Control Toolbox For Use with Matlab" *The Mathworks*, 1995.

[15] Branch, M.A., and Grace, A., "MATLAB® Optimization Toolbox User's Guide",*Version 1.5,*, The Mathworks, 1996.

[16] Srinathkumar, S., "Eigenvalue/Eigenvector Assignment Using Output Feedback," NASA Technical Paper 1118, Langley Research Center, Hampton, Virginia, February 1978.

[17] Andry, A.N., Shapiro, E.Y., and Chung, J.C., "Eigenstructure assignment for linear systems," *IEEE Transactions on Aerospace and Electronic Systems,* 19, pp. 711–729, 1983.

[18] Sobel, K.M., and Lallman, J.F., "Eigenstructure Assignment for the Control of Highly Augmented Aircraft" *J. of Guidance ,Control, and Dynamics,* Vol. 12, No. 3, May-June 1989.

[19] Klema, V.C., and Laub, A.J., "The Singular Value Decomposition: Its Computation and Some Applications" *IEEE Trans on Automatic Control,* Vol. AC-25, No. 2, April 1980, pp. 164-176.

[20] Sobel, K.M., and Shapiro, E.Y., "An Extension To The Pseudo Control Strategy With Application To An Eigenstructure Assignment Yaw Pointing/Lateral Translation Control Law" *Proceedings of the* 30^{th} *Conference on Decision and Control,* Brighton, England, December 1991.

[21] Kautsky, J., Nichols, N.K., and Van Dooren, P., "Robust Pole Assignment in Linear State Feedback", *International Journal of Control,* Vol. 41, 1985, pp. 1129-1155.

[22] Sobel, K.M., Shapiro, E.Y., and Andry, A.N., "Eigenstructure Assignment", *International Journal of Control,* Vol. 59, No. 1, 1994, pp. 13-37.

[23] O'Brien, M., and Broussard, J., "Feedforward Control to Track the Output of a Forced Model", *IEEE Transactions on Automatic Control,* Vol. AC-25, No. 4, pp.851-853, Aug. 1980.

[24] Barkana, I., "Parallel Feedforward and Simplified Adaptive Control" *International Journal of Adaptive Control and Signal Processing,* Vol. 1, No. 2, pp. 95-102, 1987.

[25] Piou, J.E., 2003, *Private communication.*

[26] Gene H. Golub, Charles F. Van Loan, "Matrix Computations" *The Johns Hopkins Univ. Press, Baltimore* , pp. 141, 1996.

[27] Ben Noble, "Applied Linear Algebra" *Prentice Hall, Inc., New Jersy,* pp. 392-393, 1969.

[28] Petkovski, D., "Robustness of Decentralized Control Systems Subject to Sensor Perturbations" *IEE Proceedings,* Vol.132, Part D, No.2, pp.53-60, March 1985.

[29] Ioannou, P., Sun, J., "Robust Adaptive Control", *Prentice Hall, Inc., New Jersy* 1996, Page 76.

[30] Sobel, K.M., Banda, S.S., and Yeh, H.-H., 1989, Robust control for linear systems with structured state space uncertainty, *International Journal of Control,* **50**, 1991-2004.